THE RESTING POTENTIAL AND FIBER SIZE OF NORMAL AND DYSTROPHIC MICE MUSCLES

Frank J. Kleeman

1960

THE RESTING POTENTIAL AND FIBER SIZE OF NORMAL AND DYSTROPHIC MICE MUSCLES

by

Frank J. Kleeman

A thesis presented to the faculty of the
Yale University School of Medicine
in partial fulfillment of the
requirements for the degree of
Doctor of Medicine

Section of Neurology
Department of Internal Medicine

1960

To my wife, Susan

ACKNOWLEDGMENT

The author wishes to express his appreciation to Dr. Gilbert H. Glaser who has supplied laboratory space and equipment and who has guided this research from its beginning. He also wishes to express his appreciation to Dr. Lloyd D. Partridge and Mr. John T. Conrad not only for their help in the technical problems involved in the use of microelectrodes but also for their many excellent ideas concerning the plan, execution, and analysis of this study and above all for their constant encouragement and teaching. Thanks are also due to Mrs. Elaine Shawaker for her technical assistance and preparation of all of the histological slides.

TABLE OF CONTENTS

Page

LIST OF FIGURES

Page

LIST OF FIGURES

INTRODUCTION

In the early 1850's the first descriptions of progressive muscular dystrophy were independently published by Aran and Meyron (Tyler & Wintrobe, 1950). In 1868 Duchenne published a paper on pseudohypertrophic or myosclerotic paralysis describing the increase in connective tissue and fat cells with preservation of cross striations in the affected muscles. In 1872 he described the progressive muscular atrophy of childhood, and in 1884 Erb published an account of the juvenile form followed the next year by Landouzy and Déjerine's description of the facio-scapulo-humeral type of muscular dystrophy. Not until 1891 was the concept of a primary dystrophic disease of muscle distinguished from muscular atrophy by Erb. Since this time the pathological and biochemical changes, patterns of inheritance, and clinical syndromes of muscular dystrophy have all been described in detail (Adams <u>et al</u>, 1954). However, until recently there has been little investigation of the deranged physiology of the dystrophic muscle. This was in part due to the lack of an experimental animal in which the disease could be produced. Although vitamin E deficiency in the hamster and potassium deficiency in the rabbit cause myopathies, these are in many ways quite dissimilar to muscular dystrophy in man (West & Mason, 1955).

In 1951 Dr. Elizabeth S. Russell noted an inherited

primary myopathy that had occurred spontaneously in the Strain #129 mice at the Jackson Memorial Laboratory. The gene responsible for this disease was found to be an autosomal recessive with incomplete penetrance. The disease itself is characterized by progressive ataxia, atrophy of the hind limb musculature, dragging of the hind limbs, kyphosis, head nodding, failure to gain weight normally, and a shortened life span (see Figure #2). No central or peripheral neural pathology has been discovered in these mice, and the muscle changes are basically similar to those seen in human muscular dystrophy. Proliferation of sarcolemmal nuclei, increased interstitial tissue, variation in the size of muscle fibers, and mixed distribution of normal and diseased fibers are quite prominent on histological sections. Long chains of nuclei are commonly observed, and on cross section many muscle fibers contain centrally placed nuclei (Michelson _et al_, 1955). Very large fibers with vacuolization are seen as well as very small fibers surrounded by sarcolemmal nuclei. Few inflammatory cells are found, but there are rows of fat cells and increased amounts of fibrous tissue between muscle fibers (see Figures #21 to #28). These mice are also known to have increased excretion of creatine and diminished urinary creatinine (Banker & Denny-Brown, 1959). Although it has not been proven that this hereditary disease in the mouse is the same as progressive muscular dystrophy in man, the similarity is striking. In any case the dystrophic mouse

has provided an experimental animal in which the physiological changes that occur in this primary myopathy can be studied. Whether these changes also occur in man must be determined by further investigation.

It was the original purpose of this paper to find out if a difference in the skeletal muscle resting potential exists between the normal and dystrophic mouse. In preliminary experiments on frog muscle experience was gained in the use of conventional microelectrode techniques. However, in pilot studies of mammalian muscle it was found that many factors tended to bias the selection of resting potentials when the usual method of single penetrations of fibers was used. It was also quite apparent that to discern any real difference in resting potentials in normal and dystrophic mice, biased selection of data would have to be minimized. The technique of driving a microelectrode through an excised muscle and recording changes in voltage continuously had recently been described by Creese _et al_ (1957). It was decided to use this technique in order to reduce the difficulty of choosing which voltage changes were "true" resting potentials. Although some bias is introduced in laying down criteria for the selection of resting potentials, once these criteria are made little bias occurs in the analysis of the records; and these are examined in the same way for both the dystrophic and normal muscles. With this method and using muscles in the living anesthetized mouse, it was also possible

to estimate not only the resting potential but also the average fiber size, the fiber space, and the extra-fiber space *in vivo*. This was done in both normal and dystrophic mice. Furthermore, histological cross sections from these muscles were studied in a way that duplicated that which the microelectrode had "seen" *in vivo*. By these techniques the resting potential values were compared in living normal and dystrophic mice; and the fiber size as well as geographical distribution of fibers was studied *in vivo* and histologically.

METHODS AND MATERIALS

Animals

The experiments described in this paper utilized an *in vivo* preparation of the gastrocnemius muscle of the Jackson Memorial Laboratory Strain #129 Swiss mouse.* Both mice afflicted with hereditary muscular dystrophy and their normal littermates were used for *in vivo* studies. Intraperitoneal 1% sodium amobarbital in an initial dose of 0.01 cc. per gram of body weight plus 0.05 cc. was used for anesthesia. Increments of 0.1 to 0.2 cc. of 0.5% sodium amobarbital were used as necessary to maintain the desired depth of anesthesia. These increments were administered through an indwelling polyethylene catheter inserted into the peritoneal cavity through an 18 gauge needle and sutured in place. Prior to a microelectrode penetration, a small dose of anesthetic was given to depress respirations and movements which would interfere with electrical recording. It was noted that the dystrophic mice were especially sensitive to anesthetic agents, but oxygen given when respiratory depression was severe tended to stabilize the mice and markedly reduced the anesthetic mortality. Ether given in combination with sodium amobarbital was observed to potentiate the

---

* Purchased from the Jackson Memorial Laboratory, Bar Harbor, Maine.

METHODS AND MATERIALS

[illegible]

The experiment described in this paper utilized [illegible] in vivo preparation of the gastrocnemius muscle of the [illegible] mice afflicted with hereditary muscular dystrophy and [illegible] normal littermates were used for in vivo studies. Intraperitoneal 1% sodium pentobarbital in an initial dose of 0.01 cc. per gram of body weight plus 0.05 cc. [illegible] in subcutaneously. Increments of 0.1 to 0.2 cc. of 0.1% sodium pentobarbital were used as necessary to maintain the [illegible] depth of anesthesia. These increments were [illegible] [illegible] the peritoneal cavity through an 18 [illegible] needle [illegible] in place. Prior to a microelectrode penetration, a [illegible] dose of anesthetic was given to [illegible] movements which would interfere with the electrical recording. It was noted that the dystrophic mice were especially sensitive to anesthetic agents, but operative [illegible] respiratory depression was severe [illegible] to stabilize the mice and [illegible] reduce the anesthetic mortality. [illegible] sodium pentobarbital was [illegible] to potentiate the

---

* Purchased from the Jackson [illegible] Laboratory, Bar Harbor, Maine.

barbiturate effect and greatly endangered the animal's survival. Sodium pentobarbital and sodium thiopental were also tried, but these were not nearly as safe and no more effective than sodium amobarbital. By giving small doses of anesthetic and oxygen when necessary, the mortality from anesthesia was quite low.

When the mouse was satisfactorily anesthetized, the left side of the abdomen and the leg to be studied were shaved. The polyethylene catheter was placed in the peritoneal cavity, and the leg dissection carried out. A longitudinal incision from the heel to the mid thigh was made on the dorsal aspect of the shaved leg. The skin was separated from the fascia by blunt dissection, and the fascia was incised longitudinally to expose the gastrocnemius muscle. Sutures placed in the fascia edges were used to maintain the exposure. The mouse was transferred to the lucite mounting chamber (see Figure #3) and the dissected leg secured in the trough. During the dissection and mounting procedures special care was taken to avoid excessive bleeding and injury to the gastrocnemius muscle which was kept moistened with mammalian Ringer's solution at all times. By these techniques oxygen and nutrient materials were supplied to the muscle through the normal circulation, and as near physiological conditions as possible were maintained while the microelectrode studies were being carried out.

beneficial effect on [illegible] nearly [illegible] the [illegible] survival. So long as anaesthesia [illegible] continuation [illegible] alone [illegible], but [illegible] more [illegible] effective than [illegible] [illegible]. [illegible] of anaesthetic and oxygen when necessary, the mortality from anaesthesia was quite low.

When the mouse was settled comfortably on its back, the left side of the abdomen and the leg to be operated were shaved. The only hindlimb collateral [illegible] activity, and [illegible] the adductor [illegible]. [illegible] incision, from the knee to the [illegible], was made [illegible] femoral sheath of the [illegible]. The [illegible] were [illegible] the fascia by blunt dissection, [illegible] longitudinally to expose the [illegible]. [illegible] placed in the fascia edges [illegible] to [illegible] the [illegible]. The mouse was then [illegible] to the [illegible] (see Figure 9) [illegible] the [illegible].

Care was taken to avoid [illegible] the [illegible] muscle which [illegible] solution [illegible] Ringer's solution at 37 [illegible]. [illegible] and [illegible] the [illegible] were [illegible].

Solutions

The mammalian Ringer's solution had the following composition: NaCl 121mM., $NaHCO_3$ 25.0mM., KH_2PO_4 0.54mM., KCl 4.75mM., $CaCl_2 \cdot 2H_2O$ 1.66mM., $MgCl_2 \cdot 6H_2O$ 0.23mM., Glucose 11.1mM. The glucose and $NaHCO_3$ were added to the solution immediately before it was to be used.

Microelectrodes and Holders

Micropipettes were made from five centimeter lengths of vaccine tubing 0.9 to 1.4mm. O.D. They were formed on a commercial model of the micropipette puller designed by Nastuk and Alexander (1953). By applying first a weak pull of 100 grams followed by a strong pull of 1700 grams as the glass tubing was heated within a platinum loop, micropipettes with tip diameters of less than 0.5u. were produced. These micropipettes were placed on a moist glass microscope slide and bound in place with white cotton thread. The glass slide was then immersed in a vertical position (micropipette tips down) into 95% ethanol. A vacuum created by a Venturi water pump caused the alcohol to boil without the application of heat (see Figure #6). After boiling gently for about 15 minutes in 95% ethanol, the slide was placed in distilled water for 1-2 minutes and then stored in a Copeland staining jar filled with 3M.KCl for at least 3-4 days after which the micropipettes were ready for use. Storage in a sealed Copeland staining jar filled with 3M.KCl with the slide in a vertical

position and the micropipette tips down could be carried out for many weeks or months without damage to the micropipettes. Many different methods of filling micropipettes were tried but none were as satisfactory as that outlined above.

Gross abnormalities of the micropipette tips could be seen with the light microscope, but since resolution is possible only to about 1 u., tips with diameters of less than 0.5u. were not visualized. The approximate tip size had to be determined by measurement of the microelectrode resistance to the passage of current which is roughly correlated with tip diameter (Nastuk and Alexander, 1953). Final determination of the micropipette's ability to measure resting potentials was found only by actual trial. During the procedures of pulling, filling, and storing of the micropipettes, care was taken to avoid all unnecessary handling or trauma to them as the tips are extremely fragile. By adhering to the technique described above, microelectrodes of less than 0.5u. tip diameter with junction potentials less than 10mv. and resistances of 5 to 30 megohms were produced quite consistently.

When a slide of micropipettes was to be used, it was carefully removed from its Copeland jar and placed in a Petri dish filled with freshly filtered 3M.KCl. Before each micropipette was placed in the microelectrode holder, it was rinsed briefly in distilled water to remove the excess KCl.

When used to measure resting potentials the filled micropipette was held in a lucite cylindrical holder* which

---

* Purchased from Mr. Andrew Pfeiffer, Old Lyme, Connecticut.

was about 10cm. long and 0.5cm. in diameter (see Figure #9). At each end metal fittings accommodated the microelectrode and the output Ag-AgCl wire. The holder was filled with Ringer's solution of the same composition as that surrounding the muscle, and it was made watertight by plastic gaskets between the tube and metal fittings. Electrical connection was made from the Ringer's solution to the cathode follower by means of a Ag-AgCl wire that was insulated with a tight-fitting polyethylene tube as it passed through the upper metal fitting of the holder. A rinsed micropipette was placed through the central hole of the lower metal fitting which was then screwed tight to hold the micropipette in place. Care was taken to prevent an air bubble from remaining above the micropipette when it was placed in the holder as this would distort the resistance of the system.

An identical lucite tube with a matched Ag-AgCl wire and filled with the same Ringer's solution was used for the indifferent electrode (see Figure #7). However, the bottom metal fitting and micropipette were omitted; and the lucite tube dipped directly into the solution bathing the muscle.

Paired Ag-AgCl wires were produced from 20cm. lengths of silver wire which was electroplated in dilute saline solution. A 5cm. long spiral was made at one end of each wire by wrapping the wire around the shaft of a 27 gauge lumbar puncture needle. This spiral plus about 5cm. of wire as about 1.5 [illegible] in diameter ([illegible]). At each end small fittings [illegible] of [illegible] and the outlet [illegible]. The [illegible] was filled with Ringer's solution of the same concentration [illegible] the muscle, and it was made tight [illegible] between the tube and metal fittings. [illegible], was made from the Ringer's solution [illegible] by means of a [illegible] wire that [illegible] fitting polyethylene tube as it [illegible] the [illegible] fitting of the holder. [illegible] microelectrode [illegible] through the central hole of the lower metal fitting [illegible] was then covered [illegible] to hold the [illegible]. Care was taken to prevent air bubbles [illegible] the microelectrode when it was placed [illegible] would disturb the [illegible] of the [illegible].

An identical lucite tube with [illegible] and filled with the same Ringer's solution [illegible] indifferent electrode ([illegible]). However, [illegible] metal fitting and microelectrode were omitted and the [illegible] tube dipped directly into the [illegible].

[illegible] silver [illegible] of silver wire which [illegible] solution. [illegible] also by [illegible] results. [illegible] was cleaned by dipping it in concentrated nitric acid. The unwound end of each wire was connected to the anode of an electroplating device, and a plain piece of silver wire was attached to the cathode. The parts of the wires to be plated were immersed in dilute NaCl solution, and current was allowed to flow until the spirals became uniformly grey-black in color. This usually took about 15 minutes at 1.0 to 1.5 volts. The Ag-AgCl spirals were then inserted into the lucite holders care being taken to avoid damaging the AgCl coating. The electroplating device used for this work caused chloride ions to be plated on the silver wire for 50 seconds and reversal of current for 10 seconds. This presumably gave a more uniform layering of chloride ions, but a 1.5 volt dry cell connected so that chloride ions will flow continuously to the spiral silver wires (anode) is probably just as effective.

The voltage between paired Ag-AgCl wires was tested after electroplating and before each experiment to determine if significant polarization had occurred. Studies using a Leeds and Northrup Type K Potentiometer to measure accurately the voltage between Ag-AgCl wires were carried out. These showed that immediately after electroplating the voltage between paired wires was generally less than 0.5mv. If square wave pulses of 100mv. with a duration of 1.5msec. and frequency of 20/sec. were passed through the Ag-AgCl wires for 10 seconds, there was little detectable change in the was cleaned by dipping it in concentrated nitric acid. The opposite end of each wire was connected to the [illegible] of a [illegible], and a [illegible] was attached to the cathode. The ends of the wires to [illegible] were immersed in dilute HCl solution, and current was allowed to flow until the area [illegible] color. This usually took about 15 [illegible] at 1.5 [illegible] volts. The Ag-AgCl spirals were then [illegible] care being taken to avoid [illegible]. The electrolytic device used for this work [illegible] to be [illegible] the silver wire for 5 [illegible] reversal of current for 10 seconds. This [illegible] more uniform layering of [illegible], but [illegible] cell connected so that chloride [illegible] to the enamel silver wire (anode) [illegible] effective.

The voltage between [illegible] 1.5-1.7 [illegible] electrolysis [illegible] of [illegible]. [illegible] were [illegible]. [illegible] that [illegible] of 300 [illegible] of [illegible] 10 seconds, [illegible] voltage between wires. Therefore, if voltages of more than 2-3mv. were found between paired Ag-AgCl wires, these were discarded and new ones made.

Micromanipulator

The lucite cylinder holding the micropipette was mounted on the vertical movement of an old microscope from which the stage and barrel had been removed (see Figure #9). The fine adjustment of the microscope was used to move the microelectrode over a total distance of 2.6mm. through the muscle. Calibration of the fine adjustment knob made it possible to move the microelectrode 35u. every 10 sec. by manually turning this knob. This technique was used in pilot experiments. But in later experiments on normal and dystrophic mice a belt connected between the fine adjustment knob and a 1 R.P.M. motor drove the microelectrode through the muscle at a uniform speed of about 2.3u./sec. Thus the full range of 2.6mm. was covered in 15-20 minutes. A make and break switch attached to the motor was used to activate a pen marker on the Bristol recorder. This provided a mark on the record for every quarter revolution of the motor which corresponded to advancement of the microelectrode tip through a distance of 35u. in the muscle.

Recording Apparatus (see Figures #4, 5, 7, and 8)

A change in voltage which appeared at the tip of the

microelectrode (compared to the indifferent electrode) was transmitted through the 3M.KCl in the micropipette, through the Ringer's solution in the holder, and along the Ag-AgCl wire to the cathode follower. Since the glass micropipette filled with 3M.KCl has a very high resistance to current flow (about 10-20 megohms), an impedance matching device such as a cathode follower had to be used to prevent signal distortion. Various designs are available, but two were found to be most useful. The first one (see Figure #10) employed a 6AK5 tube which was selected for grid current of less than 10^{-10} amps. to prevent depolarization of the muscle cell and distortion of the signal. During the winter the 6AK5 tubes with grid currents less than 10^{-10} amps. remained in this range, but in warmer and more moist weather the grid current increased markedly. Therefore, a second cathode follower (see Figure #11) was designed using a CK5886 electrometer tube which maintained a grid current of 10^{-12} to 10^{-13} amps. In both cathode followers the Ag-AgCl wire from the microelectrode connected to the grid of the tube via an insulator on the cathode follower case. The output from the cathode follower was taken at a null point in the cathode circuit. The filament voltage of the CK5886 electrometer tube was maintained at 50 to 60% of its rated value. This did not appear to cause distortion, and it greatly increased the stability of the cathode follower.

The signal from the output of the cathode follower was [illegible] ([illegible]) was [illegible] through the [illegible], and the [illegible]'s solution in the boiler, [illegible] to the [illegible] followed. [illegible] the [illegible] filled with [illegible] has a very high resistance to current flow (about 10^{10} [illegible]), [illegible] a cathode follower had to be used to prevent [illegible]. Various designs are available, but [illegible] to be most useful. The first one (see Figure 11) [illegible] tube which was selected for [illegible] of 10^{-10} amps. to prevent [illegible] of the [illegible] distortion of the signal. [illegible] with grid currents less than 10^{-10} amps. [illegible], but in [illegible] and [illegible] point [illegible]

[illegible]

(see Figure 12) [illegible] constant [illegible] which maintained [illegible] current of [illegible]. In both cathode followers the [illegible] connected to the [illegible] of the [illegible] cathode follower [illegible]. The output [illegible] was taken [illegible] point in the cathode [illegible]. The [illegible] voltage of the [illegible] electrometer tube [illegible] 10 to 10% of the [illegible] value. [illegible], and it [illegible]

[illegible]

The [illegible] from the output of the [illegible] simultaneously recorded by a Bristol Model 560 Dynamaster pen recorder and a Waterman oscilloscope. As the pen recorder had a very slow response time, the oscilloscope was used to monitor rapid changes in voltage. Because the gain of the amplifier in the Bristol recorder was too large, a voltage divider was placed in its input circuit providing a means of adjusting the gain of the pen recorder. This direct writing pen recorder made a permanent record in graphic form of variations in voltage that occurred as the microelectrode was driven through the muscle. A second pen on the Bristol recorder, activated by a separate curcuit, recorded the depth of the microelectrode in 35u. intervals on the same chart synchronously with the voltage record. This pen was triggered by a switch on the motor that drove the microelectrode.

To accurately calibrate the records on both the Bristol recorder and the oscilloscope, a voltage calibrator (see Figure #12) was designed. This was inserted between the indifferent electrode and ground. It provided either a direct path for the signal to ground or changed the voltage of the whole circuit 5, 50, or 500mv. above or below ground potential. The output of the calibrator was originally standardized against an Eplab Standard Cell of 1.0183 volts using the Leeds and Northrup Type K Potentiometer.

To determine the resistance of the microelectrode, a shielded wire from the input of the cathode follower

provided the input to a resistance tester (Figure #13). In this device a known voltage was applied across a known resistor in series with the microelectrode and ground. The input to the cathode follower was taken between the known resistor and the microelectrode. When the known resistance was equal to that of the microelectrode, one half of the voltage appeared across the resistance and one half appeared across the microelectrode. If then the resistance was shunted, the full voltage appeared across the microelectrode. These voltage deflections were observed on the oscilloscope and Bristol recorder. Different known resistances were substituted until the voltage drop across the resistor was equal to one half of the total voltage drop.

Grid current was determined by noting the difference in voltage as seen on the oscilloscope or Bristol recorder when the cathode follower input was alternately shunted to ground through a 90 megohm resistance and to ground through no resistance. The difference in voltage is proportional to the grid current since by Ohm's law I = E/R where R = 90 megohms. Measurement of grid current was made only when the micropipette was out of the Ringer's bath. Otherwise its resistance would have been in parallel with the 90 megohm test resistor and the resultant voltage would have been altered.

To reduce extraneous noise and signal distortion, the cathode follower was mounted on the micromanipulator, and the Ag-AgCl wire from the microelectrode to the cathode follower

input was kept as short as possible (see Figure #9). Also the preparation, micromanipulator, and cathode follower were mounted in a shielded box to prevent electrical interference. However, no effort was made to achieve a very low time constant; nor were extreme measures taken to reduce capacitances as action potentials were not studied; and the time constant is not critical in the measurement of resting potentials.

Testing of the Apparatus

Prior to the beginning of each experiment, several tests for the proper functioning of the electrical equipment were made. First the Bristol recorder and oscilloscope were calibrated with a known voltage. Next without a micropipette in place the voltage between the two Ag-AgCl wires was noted by grounding the input to the cathode follower. Thirdly the micropipette holder was raised out of the Ringer's solution, and the grid current was measured. A micropipette was then selected, rinsed in distilled water, and inserted into the holder. The tip was immersed in the Ringer's bath, and the microelectrode's resistance and junction potential were determined. The junction potential is a voltage that develops between the microelectrode and ground. It is probably due to the unequal diffusion of ions at the microelectrode's tip, and it may increase when debris collects on the tip and clogs it (Adrian, 1956). The junction potential was measured by

noting the voltage change when the cathode follower input was grounded while the microelectrode was in place and its tip was in the Ringer's bath. No microelectrode was used for recording resting potentials whose resistance was below 5 megohms or above 40 megohms or whose junction potential was greater than 10mv. No correction was made for the junction potential as it would change quite unpredictably, and no method was available to determine its value while a penetration of a muscle was in progress.

If all of the above tests were satisfactory, the preparation to be studied was placed beneath the microelectrode; the indifferent electrode and a thermometer were put into the surrounding Ringer's solution; and the temperature was noted. The microelectrode was then lowered toward the muscle perpendicular to its surface with the coarse adjustment of the micromanipulator until its tip had just penetrated the first cell as shown by a sudden marked change in voltage on the oscilloscope and Bristol recorder. The motor was then started and, turning the fine adjustment knob via a belt, drove the microelectrode through the muscle. When the microelectrode had moved 2.6mm. (end of fine adjustment movement), or if there was evidence of breakage of the microelectrode, the motor was stopped; the microelectrode withdrawn from the muscle; and its resistance and junction potential measured. If the junction potential had risen, it was assumed that the microelectrode was "clogged." If the resistance

had fallen, it was assumed that the microelectrode was broken. In either case the micropipette was discarded, and a new one was placed in the holder for the next penetration. Immediately before each penetration the resistance and junction potential were measured. If they did not satisfy the above criteria, the micropipette was replaced until one was found that did satisfy these criteria.

Histological Procedures

In studies of the resting potential in normal and dystrophic mice, following the electrical recording, the gastrocnemius muscle was carefully resected and fixed in Helly's solution for 3 to 12 hours. It was then washed in water, dehydrated in increasing concentrations of ethanol, and stored for a short time in cedarwood oil. Next it was imbedded in parafin, sectioned, and stained with hematoxylin and eosin.

Slides prepared in this manner were examined under a light microscope. A calibrated optical micrometer was used to determine fiber chords under the high dry objective (430X magnification). In muscles from normal mice three sections and in muscles from dystrophic mice six or seven sections were randomly selected from the slides of each muscle for examination. The optical micrometer was adjusted so that its scale was parallel to the movement of the mechanical stage. A point near the central part on the [illegible], it was assumed that the electrodes were [illegible]. [illegible] [illegible], [illegible] one was placed in the holder for the next implantation. Immediately before each implantation the resistance [illegible] potential were measured. [illegible] they did not satisfy [illegible] criteria, the electrodes [illegible] that did satisfy these criteria.

Histological Techniques

In order [illegible] of the [illegible] of the [illegible] electrode site, following the electrolytic lesion, gastrocnemius muscle was carefully [illegible] Kelly's solution for 3 to 12 hours. [illegible] water, dehydrated in increasing concentrations of alcohol, and stored for a short time in [illegible] oil. [illegible] embedded in paraffin, sectioned, and stained with [illegible] and eosin.

[illegible] in this study [illegible] light microscope, [illegible] to determine [illegible] (20 magnification). The [illegible] and [illegible] were [illegible] selected for [illegible] used for [illegible] so that the [illegible].

external surface of the muscle was chosen, and the chord of all fibers along a straight line from this point to the internal surface were measured. Also the total distance across the muscle at the selected point was measured. By this method the muscle was examined histologically in a way that duplicated what the microelectrode had measured *in vivo* (electrically) as far as fiber size and fiber relationships are concerned. This provided a means of comparing muscle structure as seen on histological section with that determined from electrical records measured in the living mouse.

Statistical Procedures

Determinations of means, standard deviations, standard errors of the mean, standard errors of the difference, T-ratios, etc. were done according to the methods and equations described in *Elementary Statistics* by Underwood, B.J. *et al.* (1954).

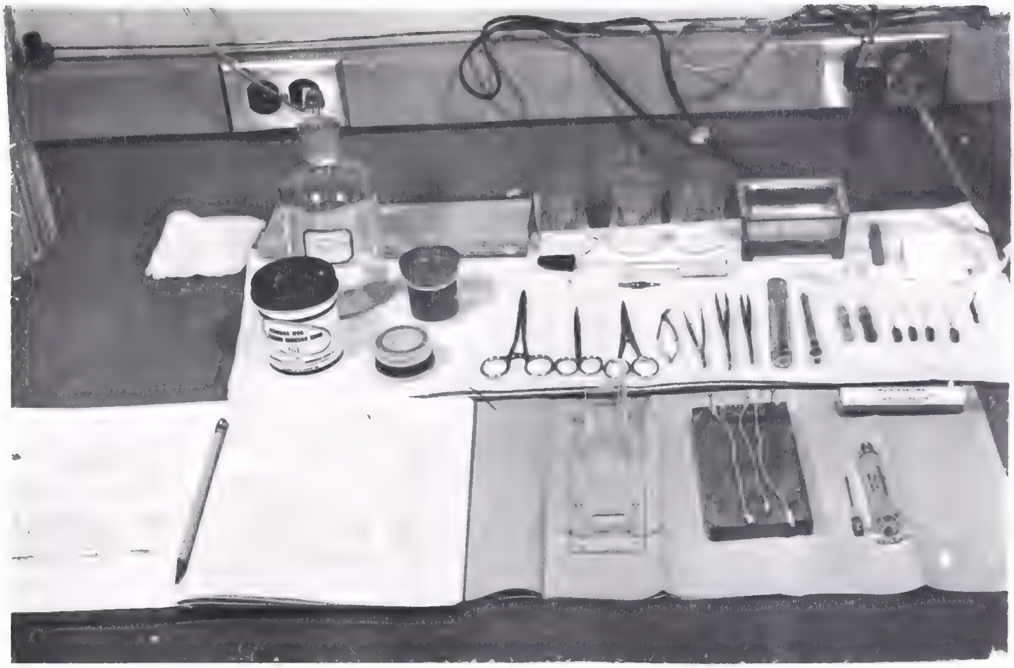

Figure #1. Mounting chamber and instruments for dissection of mouse gastrocnemius muscle.

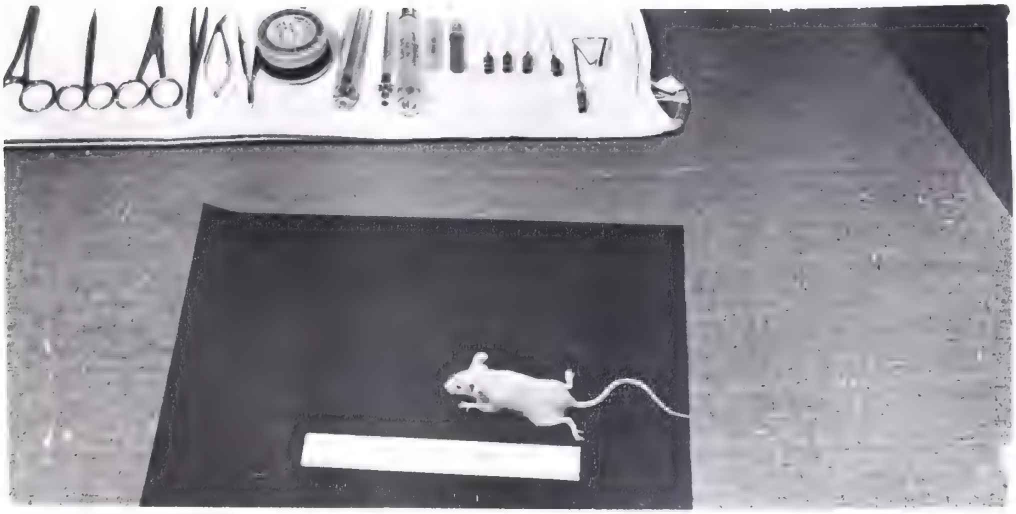

Figure #2. Living dystrophic mouse. Note position of hind limbs.

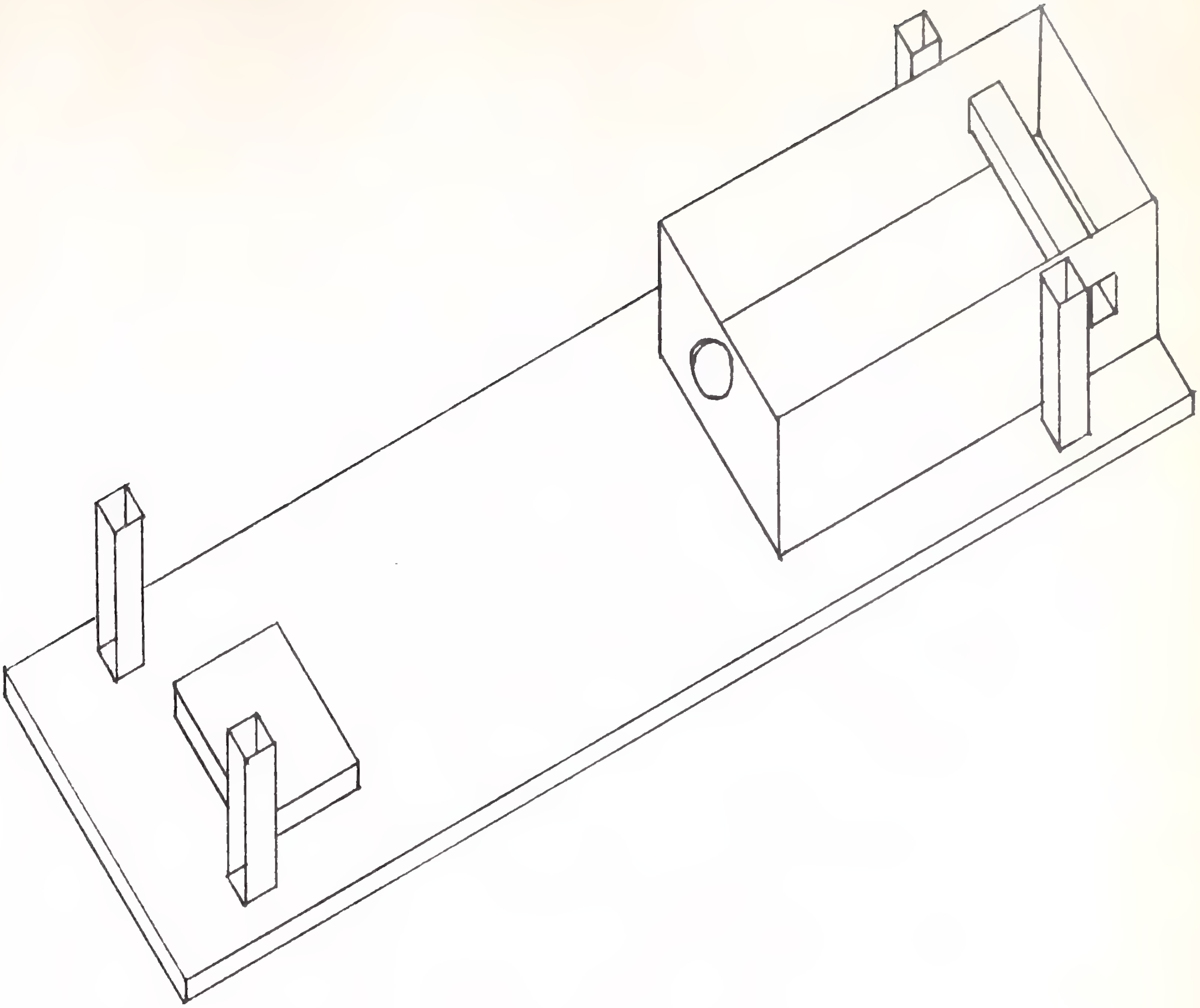

Figure #3. MOUNTING CHAMBER FOR IN VIVO STUDIES OF THE MOUSE GASTROCNEMIUS MUSCLE

The mouse's head rests on the elevated block, and its limbs are secured to three of the four corner posts. The leg to be studied passes through the hole in the trough with a string from the foot passing under the horizontal bar and secured at the back of the trough. Stay sutures to maintain exposure of the gastrocnemius are tied to the posts on either side of the trough.

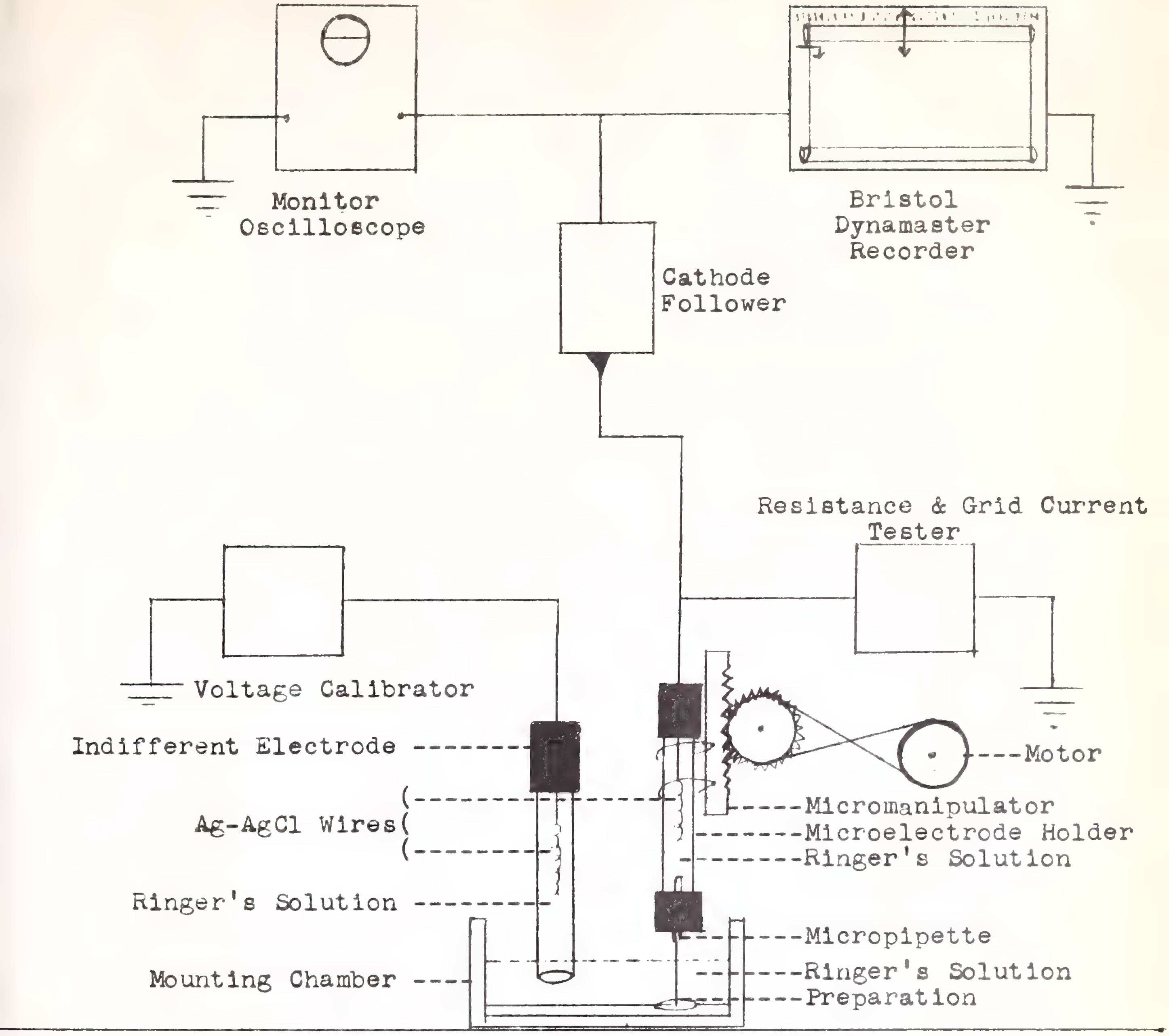

Figure #4. BLOCK DIAGRAM OF THE APPARATUS USED TO RECORD RESTING POTENTIALS

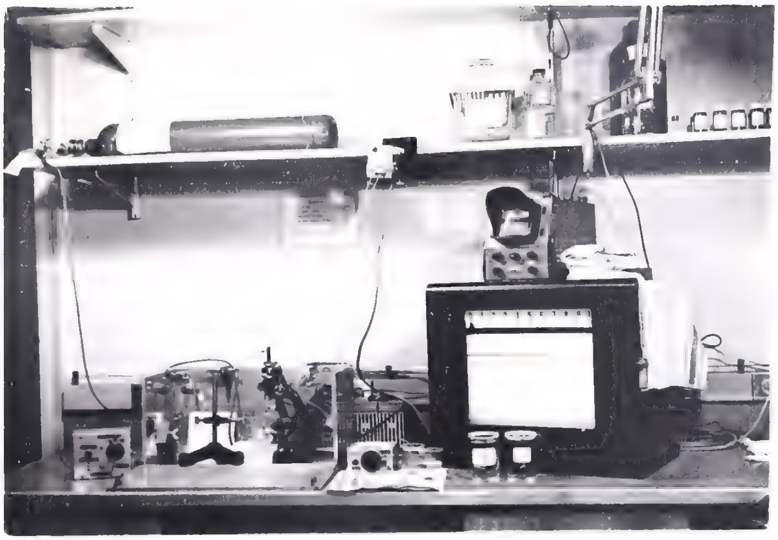

Figure #5. Electrical apparatus used to record resting potentials. Motor (attached to shelf) with belt connected to micromanipulator drives microelectrode.

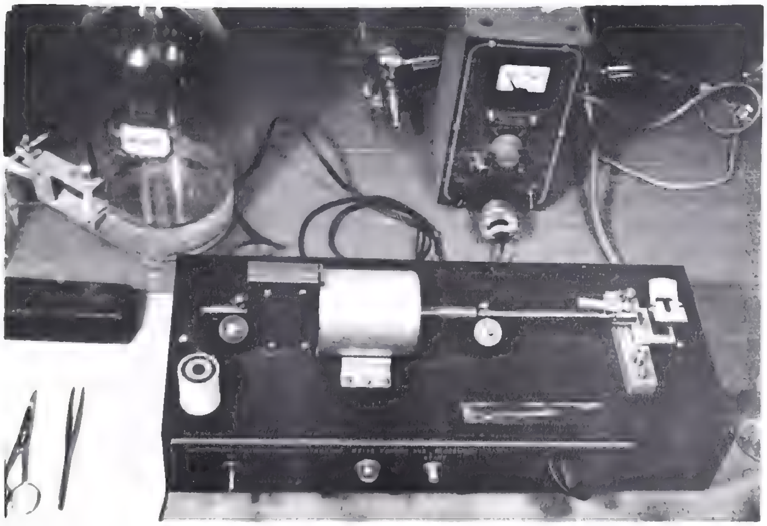

Figure #6. Micropipette puller.

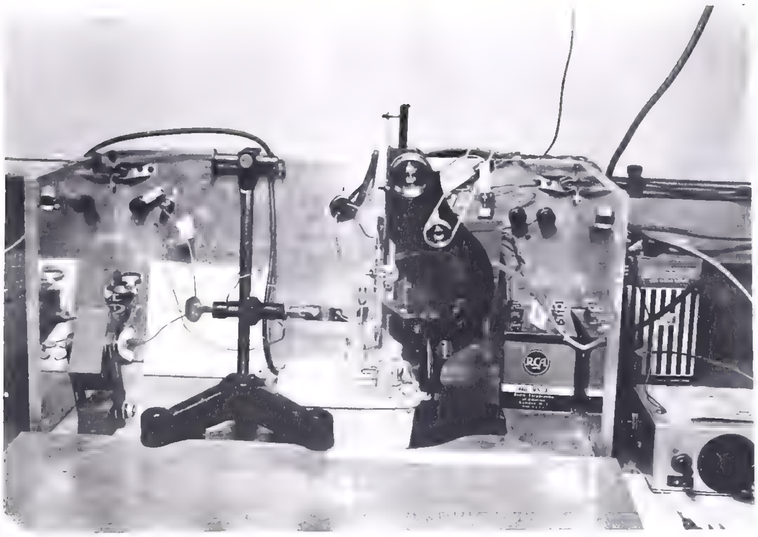

Figure #7. Micromanipulator with lucite micropipette holder. Belt from motor is attached to fine adjustment knob of micromanipulator. In left foreground is stand with indifferent electrode.

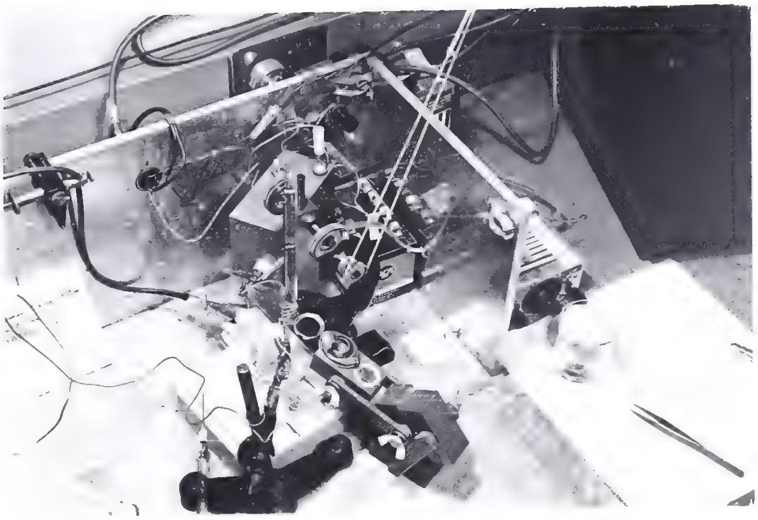

Figure #8. Recording apparatus for microelectrode impalement of in situ mouse gastrocnemius muscle. Oxygen is supplied through rubber tube and cone. Magnifying glass in center aids in placement of microelectrode.

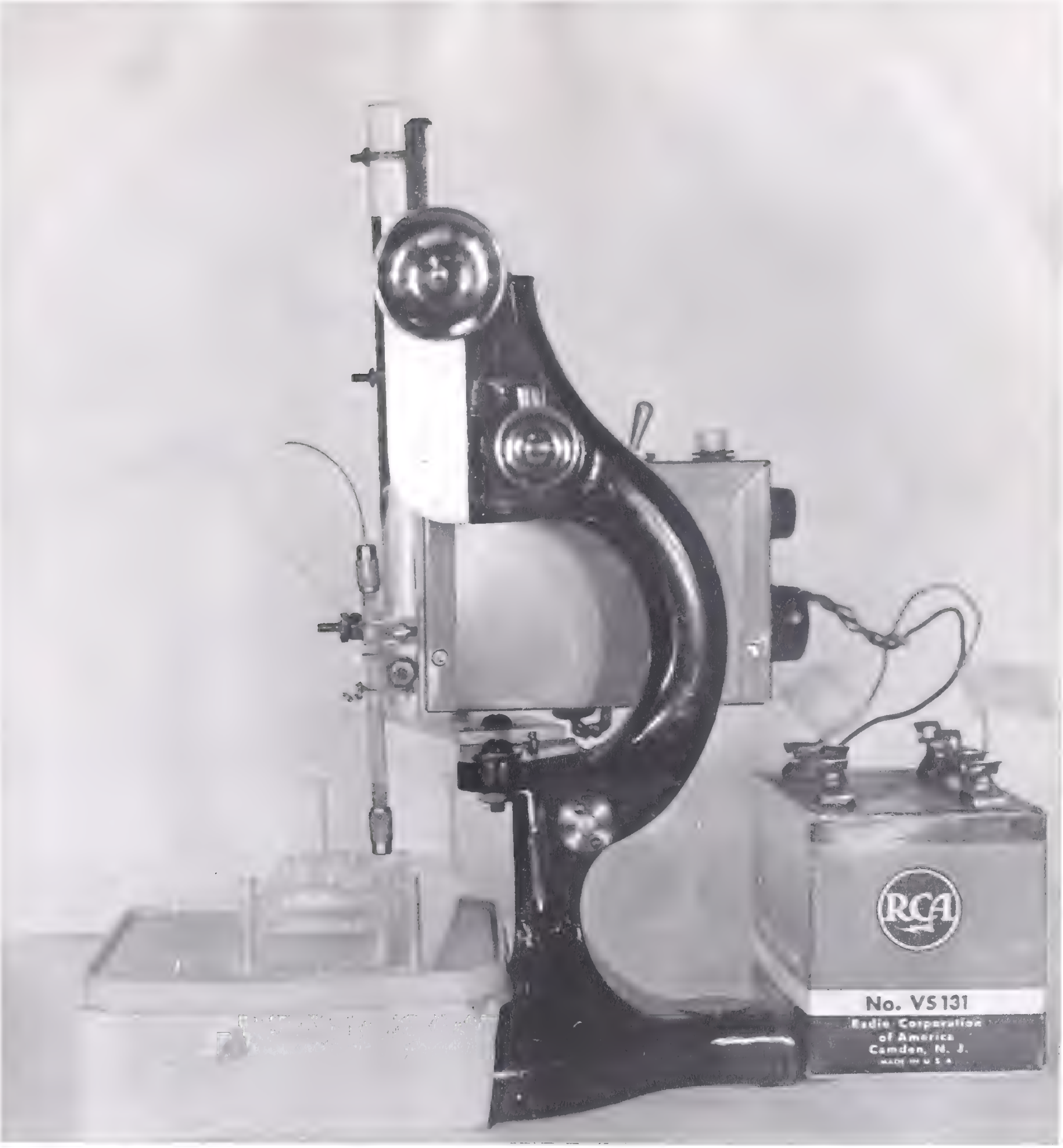

Figure #9. Micromanipulator with micropipette holder and cathode follower. Lucite chamber for mouse is in the foreground.

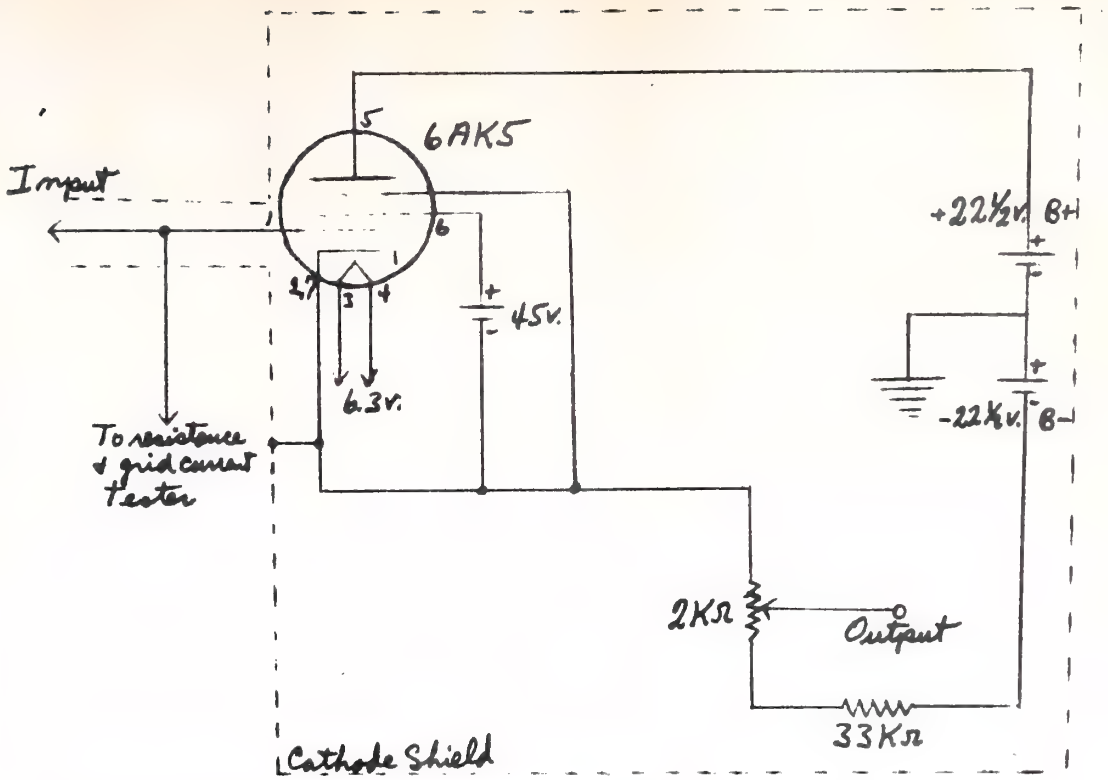

Figure #10. CATHODE FOLLOWER #1

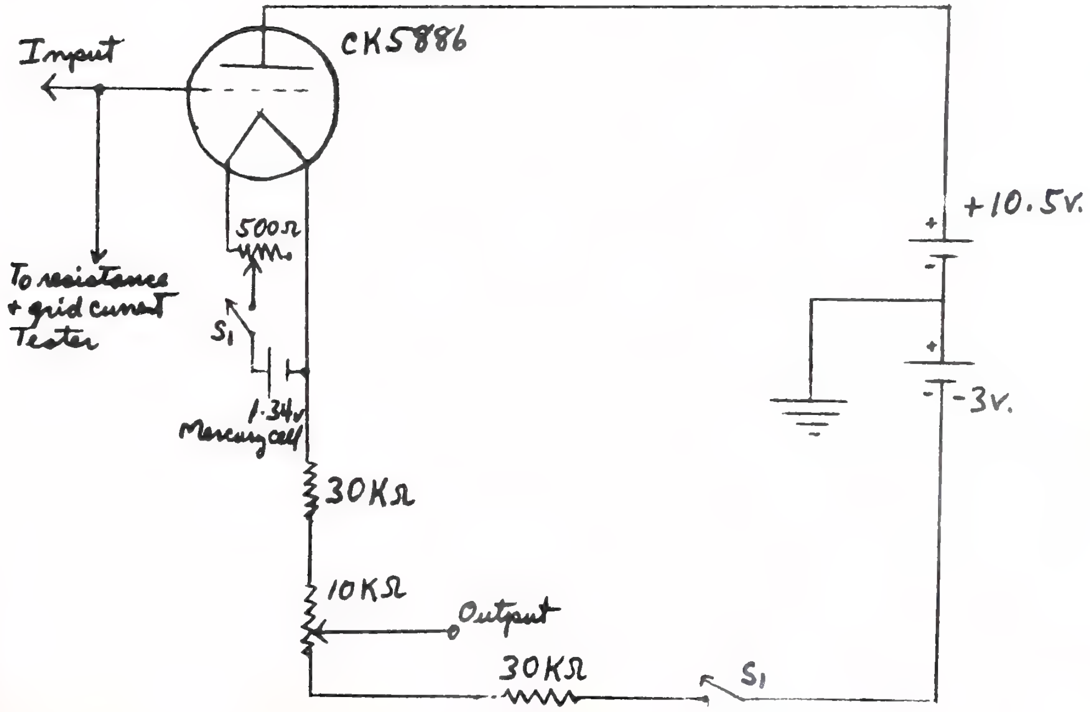

Figure #11. CATHODE FOLLOWER #2

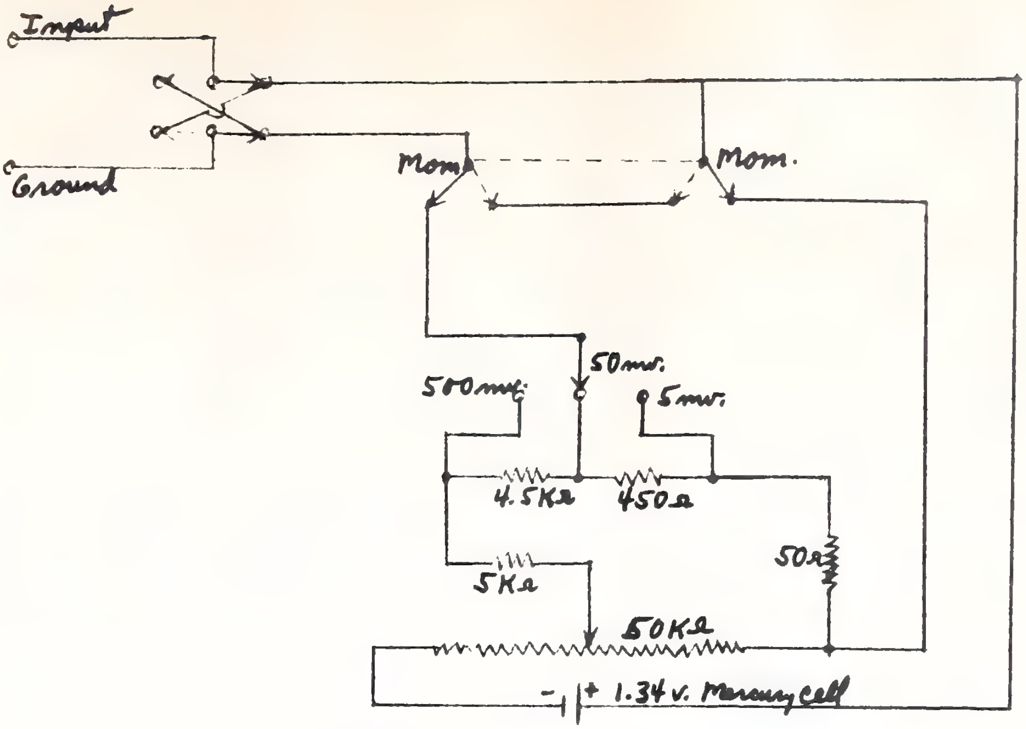

Figure #12. VOLTAGE CALIBRATOR

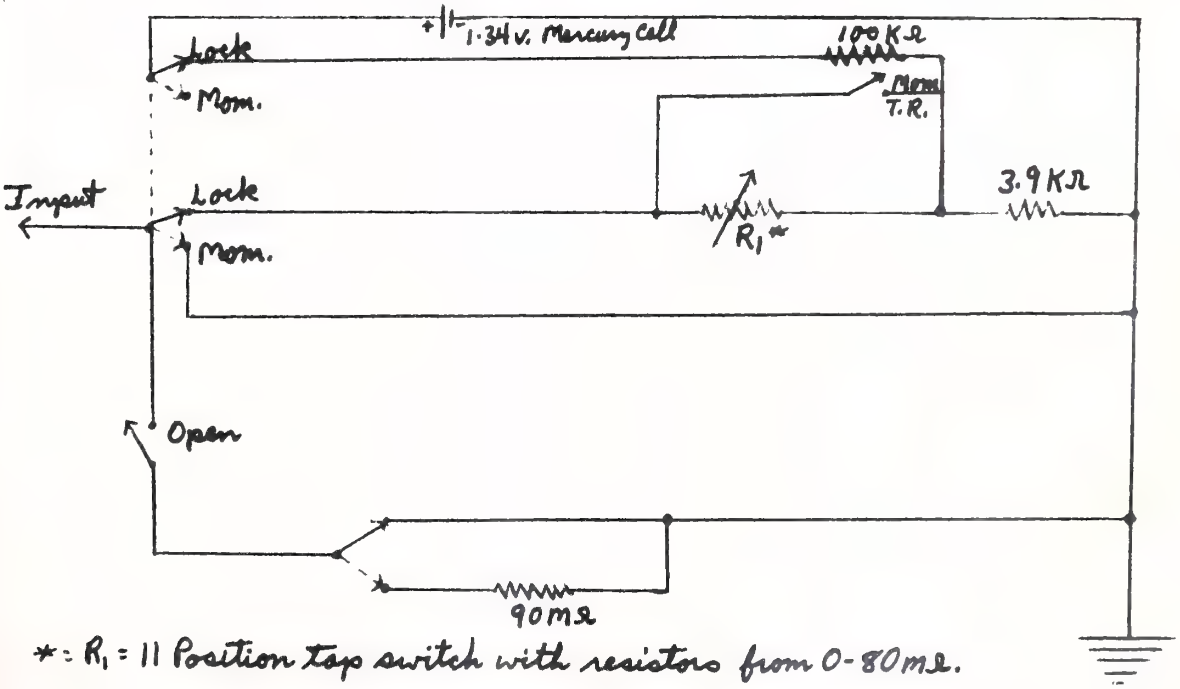

*: R_1 = 11 Position tap switch with resistors from 0-80mΩ.

Figure #13. RESISTANCE AND GRID CURRENT TESTER

RESULTS

Preliminary Studies of Normal Mice

One mouse was anesthetized with sodium amobarbital, and its right gastrocnemius muscle was exposed. Ten resting potentials were recorded by manually penetrating the muscle with a microelectrode until a sudden change in voltage (i.e., a resting potential) was noted and then withdrawing the microelectrode and repeating the procedure in another place. The mean value for these ten penetrations was 80.2 ± 6.4mv. (S.D.). The incision was closed, and the mouse was returned to its cage in good condition. Five days later the mouse was sacrificed, and in a similar manner ten resting potentials were recorded from the excised left gastrocnemius and ten from the excised right gastrocnemius muscle. The mean resting potential from the excised left gastrocnemius muscle was 74.7 ± 4.3mv. (S.D.) which did not differ significantly from the mean resting potential of the excised right gastrocnemius muscle which was 72.0 ± 4.0mv. (S.D.). Both of these values were significantly lower than the mean resting potential of the right gastrocnemius muscle _in situ_ († < 0.01). This experiment as well as other similar observations led to the choice of an _in situ_ rather than an excised preparation for resting potential measurements.

In a subsequent experiment a microelectrode was driven through a mouse gastrocnemius muscle _in situ_. It was advanced

manually 35u. every 10 seconds, and the voltage was continuously recorded. After the first penetration through the muscle, the mouse died apparently from the overenthusiastic use of sodium amobarbital. Further penetrations through the muscle were made one hour and three and a quarter hours after death had occurred. Analyses of the frequency distributions of voltages recorded at 35u. intervals as the microelectrode traversed the muscle are shown in Graph #1 for the living mouse and one and three and a quarter hours after death.

Studies of Normal Mice

Six gastrocnemius muscles in six living, normal, strain #129, Swiss mice were examined electrically and then excised and studied histologically. The mice weighed between 19 and 32 grams with an average of 27 grams. None of these mice had abnormal posture, ataxia, or other stigmata of muscular dystrophy. The mice were randomly selected, and the first three penetrations of each muscle were analyzed except for one mouse in which the first penetration utilized a microelectrode with a resistance of 38 megohms. The high resistance resulted in technical difficulties, and the penetration was omitted from the data. However, the second, third, and fourth penetrations of this muscle were analyzed. For the electrical studies the microelectrode was driven by a motor at about 2.5u./sec. through the *in situ* muscle. The voltage between the microelectrode tip and an indifferent

electrode in the surrounding bath was continuously recorded on the Bristol Dynamaster potentiometer. Notation of the microelectrode's progress through the muscle was simultaneously recorded at 35u. intervals on the record (see Figures #15 and 16). From these records the instantaneous voltage at intervals of 35u. was calculated. A frequency distribution of these voltages is plotted on Graph #2. This graph shows only the frequency with which a given voltage was recorded as the microelectrode traversed the muscle. It does not show actual resting potentials.

The original records were also analyzed in terms of resting potentials. A change in voltage had to satisfy the following arbitrary criteria to be called a resting potential. First the change had to be abrupt; and while the microelectrode travelled less than 20u., the voltage must have reached a value greater than 30mv. above the baseline (0mv.). Second the voltage must have remained relatively constant (± 20mv.) while the microelectrode traversed a distance of at least 14u. Third as the microelectrode appeared to leave the cell, the voltage must have fallen abruptly at least 10mv. The value for the resting potential was taken as the mean of the initial peak voltage and the voltage immediately prior to the abrupt fall. By these criteria 298 resting potentials were selected from the 18 penetrations of 6 muscles. The mean value was 92.5 ± 10.8mv. (S.D.). The average resting potential and standard deviation for each muscle is presented

in Table I. Graph #3 shows the frequency distribution of these 298 resting potentials.

By measuring on the records the distance that the microelectrode traversed between the initial rise of a resting potential and its abrupt fall, an estimate of the fiber chord along which the microelectrode passed through the cell was made. It was assumed that if the cell membrane dimpled inward as the microelectrode entered, it would be pushed outward an equal distance as the microelectrode left the cell. No correction was made in these measurements for cells pierced along chords which differed from their maximum diameter. It was, in fact, assumed that only rarely the maximum cross-sectional fiber diameter would be recorded; and generally chords would be measured. The mean fiber chord of 297 cells was 34.8 ± 19.2u. (S.D.). The average fiber chord and standard deviation for each muscle is listed in Table I. Graph #4 shows the frequency distribution of electrically determined fiber chords, and Graph #5 shows the resting potential plotted against the fiber chord for each normal muscle cell. It should be noted that in accordance with the first and second criteria for selection of resting potentials 30mv. is the lowest resting potential and 14u. is the smallest fiber chord measured in these studies.

Hematoxylin and eosin stained cross-sections of the muscles that had been studied electrically were examined (see Figures #23, 24, and 25). A straight line arbitrarily

[illegible]

In measuring, on the recordings, the distance that the microelectrode traversed between the initial sign of resting potential and the [illegible], [illegible] the cell was [illegible]. It was assumed that [illegible] of the microelectrode [illegible], [illegible] pushed [illegible] an equal distance [illegible]. To compensate [illegible] maximum diameter. It was, in fact, [illegible] the maximum cross-sectional [illegible] of 197 cells was 71.3 ± 10 [illegible] (S.D.). [illegible] for each muscle [illegible] Table 7. [illegible] and the frequency [illegible] electrically determined diameters, [illegible] resting potential [illegible] normal muscle cell. It should be noted [illegible] with the first [illegible] potentials [illegible] the smallest fiber [illegible].

[illegible]

drawn across the section simulated the path of the microelectrode through the muscle. Histological fiber chords were determined by measuring the length of the line within cell borders with a calibrated optical micrometer. All chords less than 14u. were eliminated. Thus the histological sections were examined in a way analogous to that recorded by the microelectrode. All fiber chords greater than 14u. were measured along a straight line as the line passed across cell borders in three sections from each of the six muscles studied electrically. The mean histological fiber chord of 837 cells had a value of 32.7 ± 15.9u. (S.D.). Table I presents the average fiber chord for each muscle. Graph #6 is a frequency distribution of the histologically determined fiber chords from the normal mice muscles.

The total distance that the microelectrode traversed was recorded for each of the three penetrations through each muscle. This distance averaged 7869u. per muscle. If all of the electrically determined fiber chords are added together, the fiber space can be determined. This space had a mean value of 1729u. per muscle. The fiber space subtracted from the total distance that the microelectrode had travelled was called the extra-fiber space. The mean value for this was 6140u. per muscle. The ratio of the fiber space to the total distance expressed as a per cent gave the mean % fiber space of 22% ± 5.5% (S.D.) per muscle. Likewise the ratio of the extra-fiber space to the total distance expressed as a per

cent gave a mean value of 78% ± 5.5% (S.D.) per muscle. Table II gives these values for each muscle from the electrical (in situ) records of normal mice.

Similar calculations were made from the histological studies. The total distance, fiber space, and extra-fiber space were determined for each muscle and for the whole group. From these values the mean % fiber space was found to be 62.0% ± 7.6% (S.D.) per muscle and the mean % extra-fiber space was 38.0% ± 7.6% per muscle. Table III gives the average values from the histological study of each normal muscle.

Since the mean electrically determined fiber chord is 34.8u. and the mean histological fiber chord is 32.7u., there is only a shrinkage of 6% of the fiber with fixation. However, for the purpose of calculating the shrinkage of the extra-fiber space due to fixation, it was necessary to allow for the increased fiber space present in the histological preparations. This was taken into account by assuming that the electrically and histologically determined mean fiber chords were equal and then utilizing the following equations to determine the ratio of the histological to electrical extra-fiber space.

$$\%S_I = \frac{S_I}{S_F + S_I} \times 100 \qquad \text{Equation \#1}$$

$$\frac{HS_I - \%HS_I(HS_I)}{\%HS_I} = \frac{ES_I - \%ES_I(ES_I)}{\%ES_I} \qquad \text{Equation \#2}$$

$$\frac{HS_I}{ES_I} = \frac{\%HS_I - \%HS_I(\%ES_I)}{\%ES_I - \%HS_I(\%ES_I)} \qquad \text{Equation \#3}$$

where: $\%HS_I$ = % Histological extra-fiber space.
$\%ES_I$ = % Electrical extra-fiber space.
S_F = Electrical or histological fiber space.
S_I = Electrical or histological extra-fiber space.

By this method the electrically determined extra-fiber space was calculated to be 5.8 times larger than the histologically determined extra-fiber space. There was thus an 83% shrinkage of the extra-fiber space but only a 6% shrinkage of the mean fiber chord with fixation and histological processing.

Studies of Dystrophic Mice

Six gastrocnemius muscles from five living Strain #129 mice afflicted with hereditary muscular dystrophy were studied. The mean weight of these mice was 15 grams which was significantly less than the mean of the normal mice at the 1% level ($\dagger < 0.01$). The weights ranged from 13 to 17 grams. All of the mice showed rather severe disease with dragging

of their hind limbs, head nodding, and weight loss (see Figure #2). No attempt was made to control the factors of age or weight. In situ electrical studies were carried out in a manner similar to that used for the normal mice. Following the electrical measurements, the gastrocnemius muscle was excised and histological sections prepared from it. Five or six motor driven microelectrode penetrations were made through each muscle with continuous recording of the voltage. A record was stopped when the tip of the microelectrode was found to be broken as evidenced by a drop in the resistance. Often after the microelectrode had penetrated about 1000u. or more the voltage would suddenly rise to 50mv. or higher and remain at this level while the microelectrode moved 300 to 1000u. or until the record was stopped. It was not possible to measure the microelectrode's resistance at voltages over 20mv.; but after these very long intervals at relatively high voltages, the microelectrode resistance was nearly always found to be quite low. The cause for this phenomenon was not determined. However, as it was quite apparent that the resting potential of a fiber was not being measured and since the resistance of the microelectrode was markedly diminished indicating probable breakage of the tip, the record was stopped and analyzed only to the beginning of this plateau. Figures #17, 19, and 20 show typical records from the dystrophic mice. The voltages which occurred at

intervals of 35u. were extrapolated from the records and used to plot the frequency distribution in Graph #7.

Exactly the same criteria for selection of resting potentials and electrically determined fiber chords were used for the dystrophic mice as for the normal mice. The mean resting potential for 166 fibers was 84.9 ± 15.9mv. (S.D.). Graph #8 shows the frequency distribution of these resting potentials. The electrically determined mean fiber chord for the 166 cells was 67.9 ± 49.1u. (S.D.). The frequency distribution of fiber chords is plotted on Graph #9. The resting potential of each cell plotted against its electrical fiber chord is presented in Graph #10. Table IV shows the average resting potential and average fiber chord for each dystrophic muscle.

The histologic sections of the dystrophic muscles were examined in a similar manner to those of the normal muscles (see Figures #21, 22, 26, 27, and 28). The number of sections studied was the same as the number of microelectrode penetrations made in each muscle except that in one muscle seven sections were examined because part of the cross-section was lost as a result of improper sectioning. The chords of 737 fibers were measured, and the mean value found to be 32.8 ± 16.0u. (S.D.). The average fiber chord for each muscle is listed in Table IV and the frequency distribution of all the histologically determined chords is plotted on Graph #11.

The total distance that the microelectrode travelled [illegible] 25 of 27%, were extracellular from the [illegible] to [illegible] for the [illegible] classification [illegible].

Exactly the same criteria for selection of [illegible] potentials and electrically [illegible] were used for the [illegible]. The [illegible] potential [illegible] mV ± [illegible] (S.E.). Graph [illegible] shows the frequency distribution of [illegible] potentials. The electrically [illegible] the [illegible] mV ± [illegible] (S.E.). The [illegible] of fibre [illegible] on [illegible] that of each cell plotted [illegible] is presented in Graph 15. Table IV shows the [illegible] potential and [illegible].

The histologic sections of the [illegible] examined in a similar manner [illegible] (see Figures [illegible]). The [illegible] showed was the same [illegible] of [illegible] blocks were in [illegible] sections were [illegible] to be a result of [illegible]. [illegible] fibres were measured, [illegible] M.M. (S.E.). The average [illegible] Table [illegible] correlation [illegible].

[illegible]

through each muscle, the electrically determined fiber space, extra-fiber space, % fiber space, and % extra-fiber space for each muscle appear in Table V. It will be noted that the electrically determined mean % fiber space is 24% ± 7.3% (S.D.), and the mean % extra-fiber space is 76% ± 7.3% (S.D.). The analogous histological data for the dystrophic mice is presented in Table VI from which it will be seen that the histologically determined mean % fiber space is 42.1% ± 3.4% (S.D.), and the mean % extra-fiber space is 57.9% ± 3.4% (S.D.).

Comparison of the electrically determined mean fiber chord (67.9u.) and the histologically determined mean fiber chord (32.8u.) showed that there was a 53% difference in the dystrophic mice muscles. Because of this difference the equations for determination of the change in extra-fiber space with histological processing were modified as follows:

$$2\left(\frac{HS_I - \%HS_I(HS_I)}{\%\,HS_I}\right) = \frac{ES_I - \%ES_I(ES_I)}{\%ES_I} \qquad \text{Equation \#4}$$

$$\frac{HS_I}{ES_I} = \frac{\%HS_I - \%HS_I(\%ES_I)}{2\,(\%ES_I - \%HS_I(\%ES_I))} \qquad \text{Equation \#5}$$

By this method it was calculated that the electrically determined extra-fiber space was 4.6 times the extra-fiber

[illegible]

-fiber content of fiber score, [illegible] for each muscle [illegible] in Table [illegible] the electrophoretically [illegible] 7.9% ([illegible]), [illegible] ([illegible]). The [illegible] histological [illegible] also be presented in Table VI from which it will be seen that the histologically [illegible] ± 2.4% ([illegible]), [illegible] 57.0% ± [illegible] ([illegible]).

Comparison of the electrophoretically determined [illegible] chord ([illegible]) [illegible] histologically [illegible] chord (32.9%) shows that [illegible]

[illegible] those for determination of the [illegible] histological [illegible]

$$[illegible]$$

$$[illegible]$$

[illegible]

~~space was 4.6 times the extra-fiber space~~ Space determined histologically. Thus there was a shrinkage of 78% of the extra-fiber space with fixation and histological processing.

The difference between the electrically and histologically determined mean fiber chords in the dystrophic mice is statistically significant at the 1% level ($\dagger < 0.01$). The dystrophic mean % fiber space from histological sections is significantly larger than that from the electrical studies at the 1% level ($\dagger < 0.01$). The inverse is true for the extra-fiber space. That is, the electrical mean % extra-fiber space is significantly larger than the histological mean % extra-fiber space in the dystrophic mice.

In the normal mice again the histological mean % fiber space is significantly larger than the electrical mean % fiber space while the electrical mean % extra-fiber space is significantly larger than the histological mean % extra-fiber space at the 1% level ($\dagger < 0.01$).

Comparison of the Normal and Dystrophic Mice

Graph #12 is a frequency distribution of voltages at 35u. intervals comparing the results from the normal with those from the dystrophic mice. The % frequency rather than the absolute frequency is used for the ordinate to allow for the difference in numbers in the two groups.

The mean resting potential of the normal mice muscles is significantly larger than that of the dystrophic muscles

~~space~~ [illegible] than the extracellular [illegible] lin-ically. The [illegible] of the [illegible] fiber space [illegible] direction and [illegible] significantly.

[illegible]

longitudinal direction, mean fiber space [illegible] the [illegible] significantly larger than [illegible] (p < 0.01). [illegible] fiber space [illegible] significantly larger than [illegible] at the [illegible] level (p < 0.05). The [illegible] extra-fiber space. That is, the [illegible] fiber space is significantly larger than the [illegible] [illegible] extracellular [illegible].

In the [illegible] the [illegible] fiber space is significantly larger than [illegible] [illegible] space is significantly lower than [illegible] extra-fiber space [illegible] level (p < 0.05).

Comparison of the [illegible]

[illegible]

[illegible]

at the 1% level ($\dagger < 0.01$). The frequency distribution of the resting potentials from the normal and dystrophic mice plotted on the same coordinates is presented in Graph #13.

Although by histologic measurements the mean fiber chords of normal and dystrophic mice muscles are essentially the same, by the electrical (microelectrode) measurements the dystrophic fibers are significantly larger at the 1% level ($\dagger < 0.01$). Graph #14 shows the frequency distribution of normal and dystrophic fiber chords determined electrically, and Graph #15 shows the frequency distribution of histological fiber chords for both groups.

The electrical determinations of the mean % fiber space and % extra-fiber space do not differ significantly between the normal and dystrophic muscles. However, in the histological studies the mean % fiber space in the normal mice is significantly larger than that in the dystrophic mice at the 1% level ($\dagger < 0.01$). Conversely the histologic mean % extra-fiber space is significantly smaller in the normal mice than in the dystrophic mice at the 1% level ($\dagger < 0.01$). It should furthermore be noted that whereas in the normal mouse the electrical mean fiber chord is only 6% larger than the histological mean fiber chord; in the dystrophic mice muscle the electrical mean fiber chord is 53% larger than that determined from sections.

In Table VII several measurements of the normal and dystrophic mice muscles are presented for comparison.

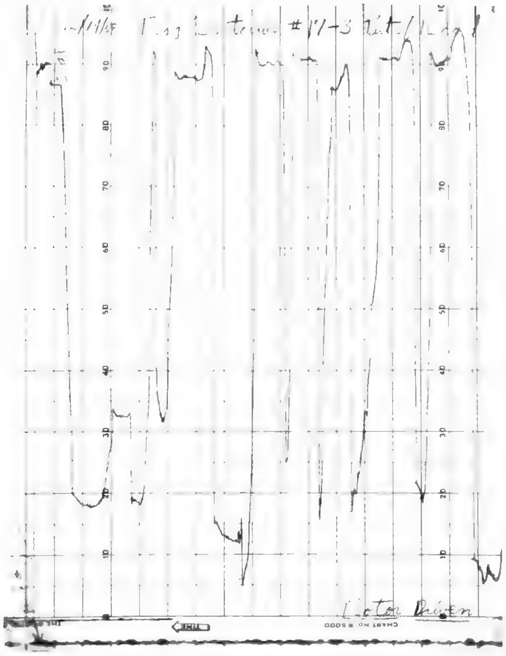

Figure #14. Motor driven microelectrode record of frog sartorius muscle. Read from right to left. Scale: lunit equals lmv. Compare with mice records.

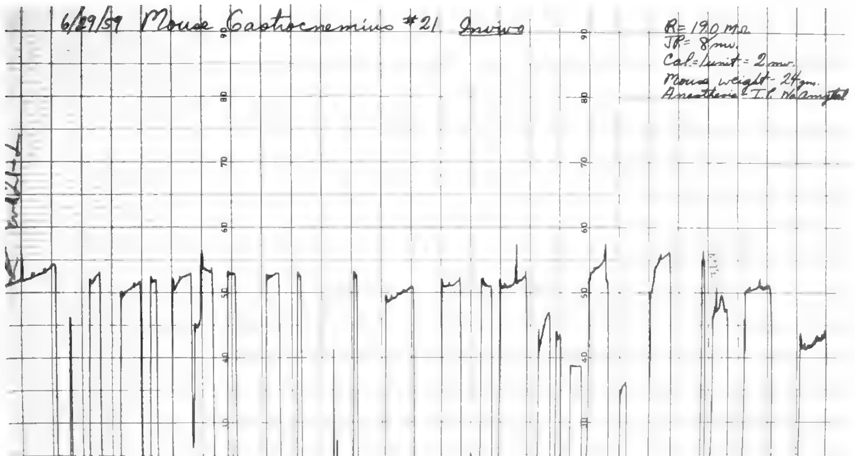

Figure #15. Motor driven microelectrode record of normal mouse gastrocnemius muscle _in situ_. Read from right to left. Scale: lunit equals 2mv.

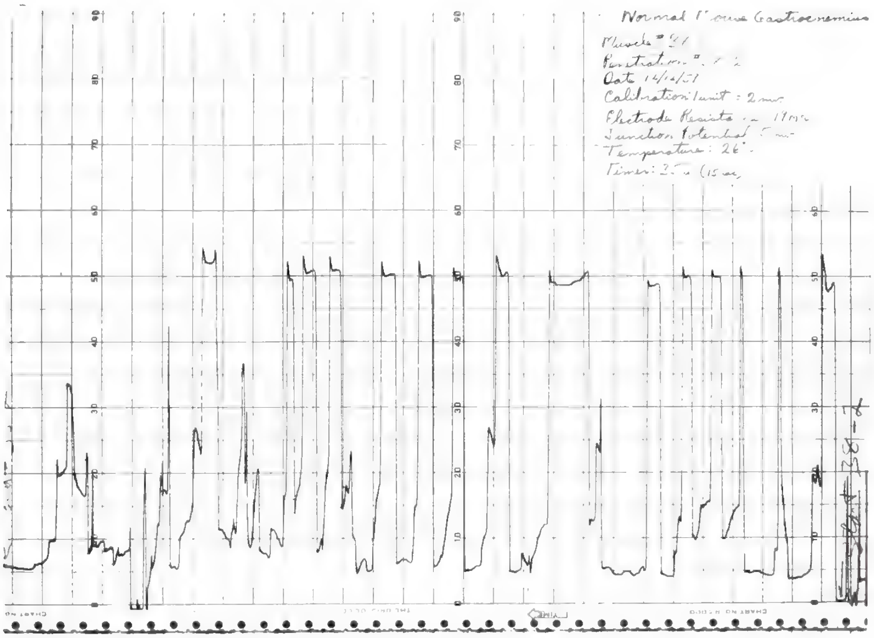

Figure #16. Microelectrode penetration of normal mouse gastrocnemius muscle. Read from right to left. Scale: lunit equals 2mv. Note uniformity of fibers and rise in resting potential before microelectrode leaves fiber. Line at bottom of record shows microelectrode depth in 35u. units.

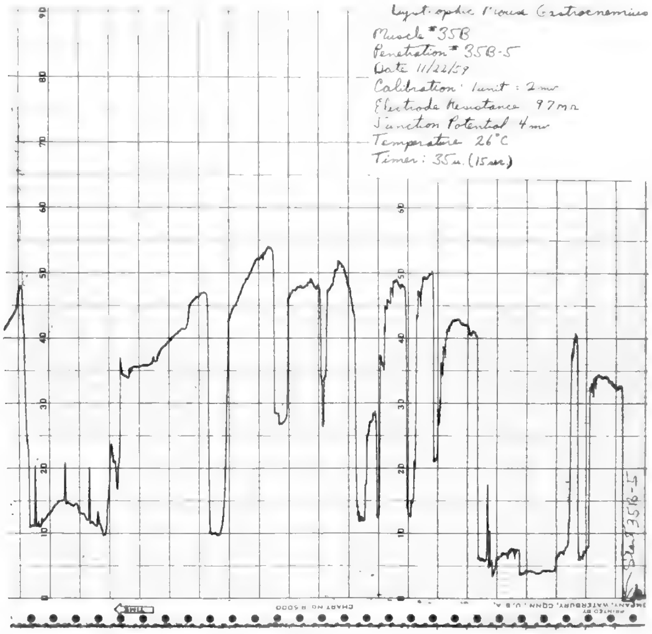

Figure #17. Microelectrode penetration of dystrophic mouse gastrocnemius muscle. Read from right to left. Scale: lunit equals 2mv. Fiber sizes and resting potentials are quite variable. Compare with Figure #16.

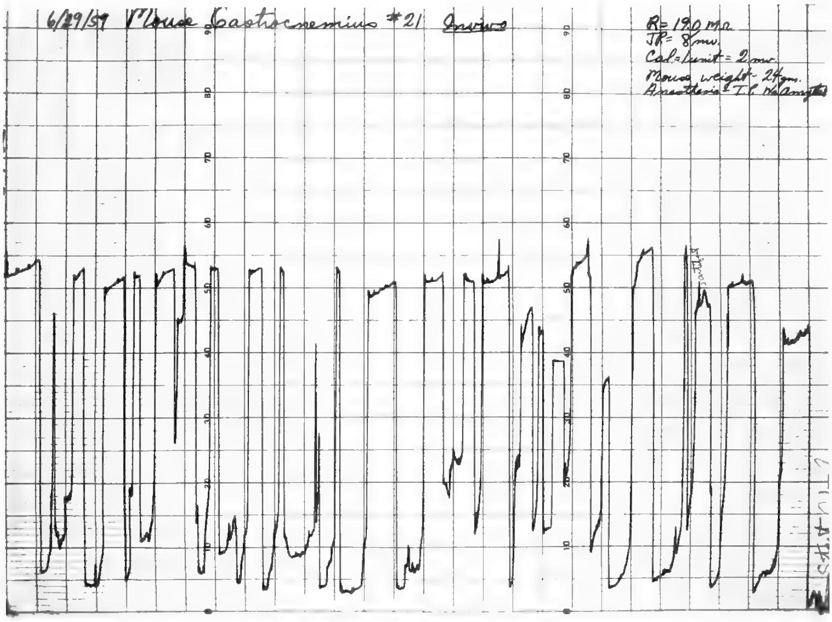

Figure #18. Normal mouse gastrocnemius record (same as Figure #15). Read from right to left. Scale: lunit equals 2mv. Compare with records from dystrophic mice below.

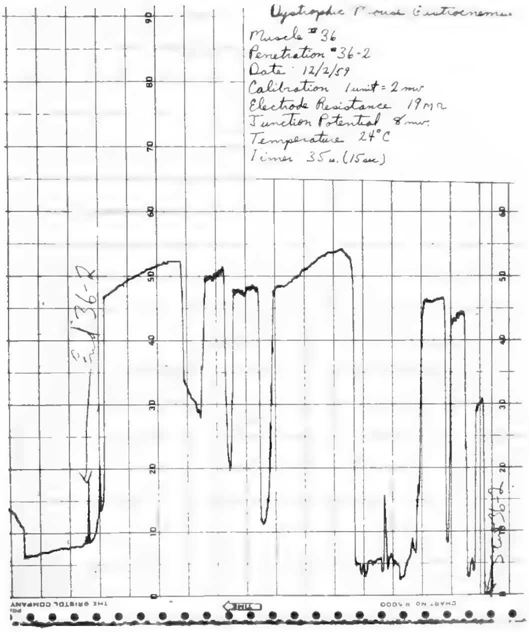

Figure #19. Dystrophic mouse gastrocnemius record. Read from right to left. Scale: lunit equals 2mv. Most fibers have normal resting potentials but are of large size.

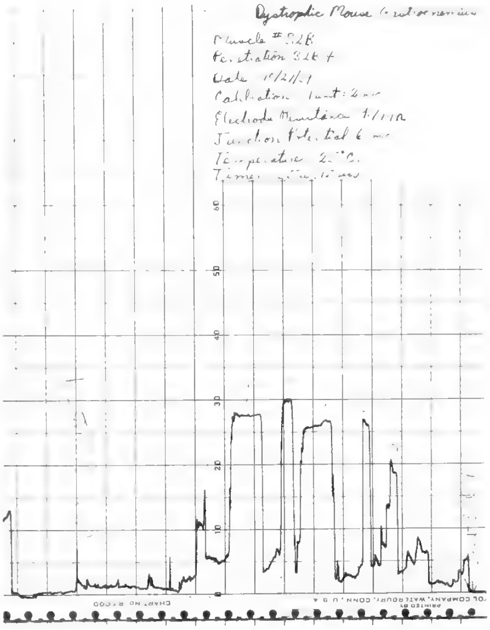

Figure #20. Dystrophic mouse gastrocnemius record. Read from right to left. Scale: lunit equals 2mv. Note small resting potentials.

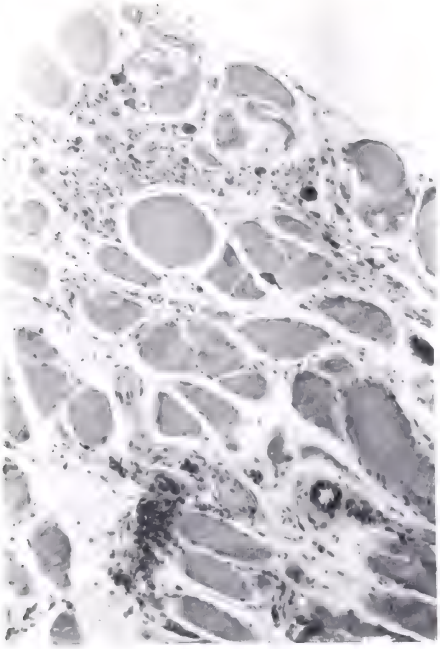

Figure #21. Dystrophic mouse gastrocnemius muscle 100X. Note sparsity of fibers compared to Figure #23.

Figure #23. Normal mouse gastrocnemius muscle 100X.

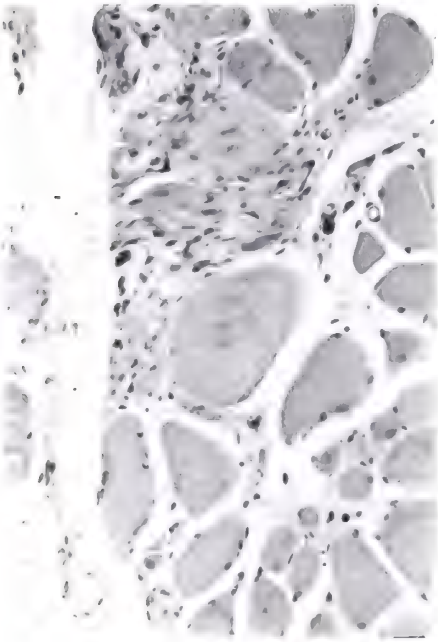

Figure #22. Dystrophic mouse gastrocnemius muscle 200X. Note central nuclei and increased connective tissue.

Figure #24. Normal mouse gastrocnemius muscle 319X.

Figure #25. Normal mouse gastrocnemius muscle 319X. Compare with Figures #26 and #28.

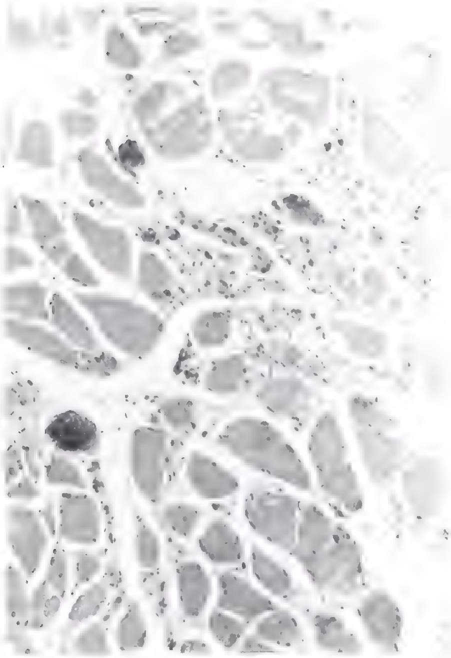

Figure #27. Dystrophic mouse gastrocnemius muscle 100X.

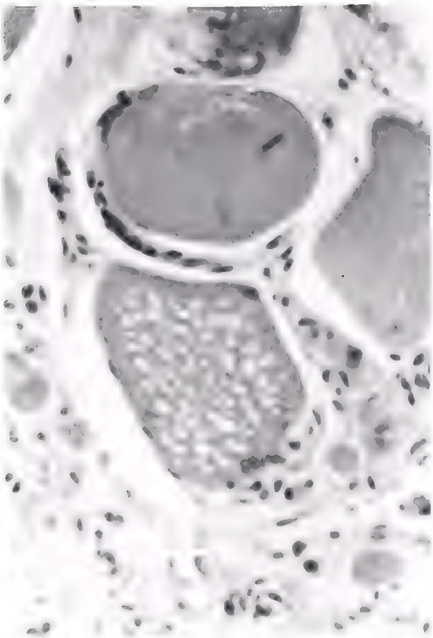

Figure #26. Dystrophic mouse gastrocnemius muscle 319X. A large vesicular fiber is in the center.

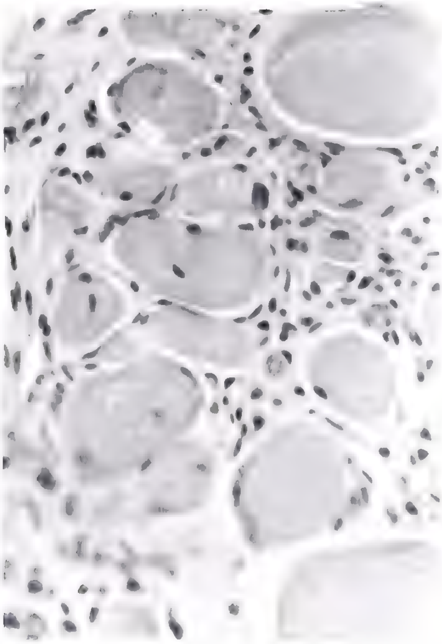

Figure #28. Dystrophic mouse gastrocnemius muscle 319X. Fibrous tissue is surrounding muscle cells.

DISCUSSION

The records from the motor driven microelectrode studies of normal and dystrophic mice were analyzed in such a way that voltages at 35u. intervals as the microelectrode traversed the muscle were determined and plotted as frequency distributions (see Grphas #2, 7, 12). This allowed for practically no selection of data by the investigator. The very low voltages are thought to have been recorded while the microelectrode was outside of cells while the peak at the higher voltages is thought to represent intracellular recording. This latter peak coincides closely with that of the resting potential frequency distributions (see Graphs #3, 8, 13). This similarity indicates that the criteria for selection of resting potentials did not materially distort the original unselected data. The motor driven microelectrode studies of the living and dead mouse (see Graph #1) serve only to show that using this technique and method of analysis, changes in the physiological state of the muscle can be measured.

For the comparison of resting potentials in the normal and dystrophic mice an <u>in situ</u> preparation was used. This was done because preliminary studies showed a significant fall in the resting potential of the excised mouse muscle, and it was thought that <u>in vivo</u> studies would be more "physiological." It is apparent from Graph #12 that between

85 and 105mv. there is a much lower frequency of voltages in the dystrophic mice than in the normal controls. But between 35 and 80mv. the frequency is higher in the dystrophic mice. A similar situation is seen with regard to the resting potential in Graph #13. From these two graphs it may be postulated that in the dystrophic muscle there are some fibers with resting potentials quite comparable to those of normal fibers. However, other fibers appear to have reduced resting potentials to varying degrees. It seems not unreasonable to propose that as the disease process proceeds the resting potential is gradually reduced to zero millivolts from its normal value of 90-100mv. If this is true, the fiber would be expected to become at first hyperexcitable as the resting potential gradually fell toward the criticial potential and later inexcitable as the voltage went below the critical potential (Jenerick and Gerard, 1953 and Jenerick, 1956). This could perhaps be the explanation for the fibrillations that have been observed in the dystrophic mice (McIntyre _et al._, 1957 and 1959).

The mean resting potential in living normal mice gastrocnemius muscles observed in this study was 92.5 ± 10.8 mv. (S.D.). This is similar to _in vivo_ resting potentials found by Bennett (1953) and McIntyre (1957) in the mouse. The following chart gives some of the resting potential values observed in mammalian skeletal muscle.

Author and Year		Preparation	# of Fibers	Mean R.P.	S.D.	Range
Bennett	1953	Mouse _in situ_	1130	99.8 mv.	6.5 mv.	79-123 mv.
McIntyre	1957	Mouse _in situ_	---	100	---	---
Choh-Luh Li	1957	Rat _in situ_	55	72.2	5.3	64-99
Boyd	1956	Cat excised	---	75	---	60-90
Liley	1956	Rat excised	31	73.2	5.2	---
Creese	1958	Rat excised	---	70-80	---	---
Zierler	1959	Rat excised	225	74	12.0	---
Creese	1957	Human excised	144	72.6	10.0	45-105

From this chart it can be seen that the excised preparation has generally a lower resting potential than that measured by _in vivo_ methods. This may in part be due to difficulty in oxygenating an excised mammalian muscle. The mean resting potential of dystrophic muscles in this study was 84.9 ± 15.9mv. (S.D.). The only mention in the literature of the resting potential in dystrophic mice muscle is an abstract by McIntyre _et al._ (1957) in which he states that the _in vivo_ resting potential of dystrophic mice is 85mv. His method, number of animals, standard deviation, and range of values are not revealed. It should be noted that in the present study the standard deviation of the dystrophic fiber's resting potentials is larger than the standard deviation for normal fibers. This is consistent with the wider spread of dystrophic muscle voltages plotted in Graph #13. Furthermore the fact

that the mean resting potential of the dystrophic muscles is significantly lower ($\dagger < 0.01$) than that found in normal muscles does not mean that there are two sharply defined groups. Rather this difference represents the admixture of normal fibers with moderately and severely diseased fibers to make up the dystrophic muscle. This combination then is sufficient to produce a statistically significant difference in the mean resting potential between the normal and dystrophic muscles. The reason for the progressive decrease in the resting potential of some fibers in the dystrophic muscles is not apparent. It may, however, be due to an abnormality in the dystrophic fiber's metabolic processes (Ling and Gerard, 1949).

During the study of the records obtained while a microelectrode was driven through a normal muscle, it was observed that in a large majority of fibers the voltage rose about five millivolts immediately before the microelectrode passed from the inside to the outside of the cell. Although this was occasionally seen in the dystrophic fibers, it was quite regularly observed in the normal records (see Figures #15 and 16). It has been commonly noted that after a muscle fiber is impaled by a microelectrode its resting potential appears to fall slowly. This has been attributed to the diffusion of ions from the microelectrode tip and to membrane injury and tearing (Nastuk and Hodgkin, 1950; Shanes, 1958; and Graham and Gerard, 1946). This fall in resting potential was often

noted in the present study especially in the normal mice records where it occasionally appeared as a mirror image of the rise in voltage which occurred before the microelectrode left the cell. It is suggested that these two observations may be manifestations of the arrangement of ions within the cell and not related to the diffusion of particles from the microelectrode or to membrane injury. The fall in voltage after the microelectrode enters a cell and the rise in voltage before it leaves the cell may be artifacts from the physical effect of the membrane on the microelectrode tip to change its resistance. This seems unlikely, however, because the voltage changes are in opposite directions. These phenomena may well represent the accumulation of negatively charged particles close to the inner surface of the membrane. Thus as the microelectrode enters the cell and passes through this layer of negative charges, the resting potential appears to fall (become more positive). After the microelectrode passes through the cell and as it approaches the opposite membrane, the resting potential rises (becomes more negative) until the microelectrode pierces the membrane and enters the extra-fiber space at which time the voltage falls abruptly toward zero. In publications by Creese _et_ _al_. (1957), Blum _et_ _al_. (1957), and Creese _et_ _al_. (1958) pictures of their records obtained with motor driven microelectrodes show the same phenomena of a fall in resting potential after the cell has been entered and a rise in voltage just before the

microelectrode leaves the cell. However, they do not comment on it. Further investigation of these voltage changes would seem justified.

In many studies of the resting potential comparison of the predicted value on the basis of known ionic constituents with the resting potential observed in the laboratory has been made. Although the predicted resting potential is rarely the same as that found experimentally, the comparison is still of interest. Using the Nernst Equation, the predicted resting potential can be calculated from the ratio of intracellular potassium (Ki) to extracellular potassium (Ko). Thus at 37°C.

$$\text{R.P.} = 61.5 \log \frac{\text{Ki}}{\text{Ko}} \qquad \text{Equation \#6}$$

According to Timiras et al. (1954) the ratio of the intracellular concentration of potassium to the extracellular concentration of potassium in mice weighing an average of 24 grams is 23. When this value is used in Equation #6, the predicted resting potential is 83.7mv. This is somewhat lower than the value of 92.5mv. obtained from the experimental studies. However, Creese (1954) found the in vivo ratio of Ki/Ko in rat diaphragm to be 34 giving a predicted resting potential of 94.2mv. which closely approximates the observed value. It has been found by Baker, Blahd, and Hart (1958) that there is a 20% reduction in the intracellular

potassium concentration of the dystrophic mice muscles as compared to the normal controls. If it is assumed that the extracellular potassium is the same in the normal and dystrophic mice, then using 20% less than Creese's ratio of Ki/Ko for *in vivo* muscle, the predicted resting potential is 88.2mv. This is slightly higher than the experimental mean resting potential of 84.9mv. for dystrophic mice muscles. The discrepancies between the predicted and experimental resting potentials could be due to inaccurate measurement of ionic concentrations, species differences, or the fact that the resting potential is not completely dependent on the ratio of intracellular to extracellular potassium.

The *in situ* fiber chord was defined as the distance that the microelectrode travelled between its entrance into and exit out of a cell as determined by changes in resting potential. The value of 34.8u. for the mean fiber chord in normal mice muscles is higher than that found by Creese *et al*. (1958) for the excised rat diaphragm. The difference between their value of 26.7u. and that obtained in this study could be explained on the basis of species variability, muscle differences, and difference in tension and angle of penetration. The large standard deviation of 19.2u. in the present study and 15.7u. in the study by Creese *et al*. (1958) is probably due in large part to the fact that fiber chords and not maximum diameters were measured. The value of the mean fiber chord measured *in vivo* is very similar to that measured from

the histological sections. The latter had a mean value of 32.7 ± 15.9u. (S.D.). Also it can be seen from Graphs #4 and 6 that the frequency distributions of fiber chords are similar in the normal mice. Therefore, the fiber shrinkage on fixation appears to be negligible. No analysis was made to convert the mean fiber chord values to fiber diameters because chords were used throughout the study for both electrical and histological observations. Emerson and Emerson (1959) found in their study of 2400 normal mouse gastrocnemius muscle fibers that the mean maximum cross-sectional fiber diameter was 48.8u. with a range of 14 to 114u. Their standard deviation was 14.7u. which is similar to that of the present study. It is to be expected that their mean maximum fiber diameter would be larger than the mean fiber chord because of the different techniques of measurement. Banker and Denny-Brown (1959) found that in normal mice muscles the fiber diameters ranged between 30 and 40u. This range is much smaller than that in Emerson and Emerson's measurements or the range of 14 to 180u. in the present study.

The dystrophic muscles had an in situ (electrical) mean fiber chord of 67.9 ± 49.1u. (S.D.). This was nearly twice as large as the in situ (electrical) mean fiber chord of the normal muscles. The large standard deviation in the dystrophic muscles is again dependent on the measurement of

chords rather than maximum diameters as well as the variability of fibers in the living dystrophic muscle (see Graphs #9 and 14). The tissue culture studies of Geiger and Garvin (1957) on muscle fibers of humans with muscular dystrophy also show that the living fibers may be very large (100-300u.). Measurements of the histologically determined mean fiber chord in the dystrophic mice showed little difference in size, standard deviation, or frequency distribution from similar measurements in normal muscles. (Mean dystrophic fiber chord is 32.8 ± 16.0u. S.D. See Graph #15). However, there was over 50% shrinkage in the mean fiber size with fixation and histological processing of the dystrophic muscle (compare Graphs #14 and 15). Banker and Denny-Brown (1959) found a range of 3 to 84u. in fiber diameters of dystrophic muscles on histological sections. The range of 14 to 130u. in the present study of dystrophic histological sections again reflects the measurement of chords rather than maximum diameters.

From the current study it can be seen that the normal muscle fiber maintains its _in situ_ size after histological fixation and sectioning. On the other hand the average dystrophic fiber _in situ_ is very much larger than the normal fiber; however, with fixation it shrinks to the same size as the normal fiber. It is apparent from Graph #14 that not all fibers in the living dystrophic muscle are larger than normal. Roughly 50% of the dystrophic fibers are of about

normal size (14-60u.); whereas about 90% of the normal fibers are in this range. In the dystrophic muscle, therefore, somewhat less than half of the fibers are larger than normal; and these range from 60 to 270u. in chord size. Whatever is present in some of the dystrophic fibers that causes them to be larger than normal in the living state is labile; and during the process of histological preparation it disappears from the fiber allowing it to shrink. Young, Young, and Edelman (1959) found that the dystrophic mouse's hind limb muscles contain twice as much total lipid as their normal littermates. In the dystrophic mouse this is about 16.4 grams per 100 grams of dry tissue; while in the normal mouse it is about 8.4 grams per 100 grams of dry tissue. This represents an increase in the dystrophic mouse muscle of only 8% of the total dry tissue, and it would be even less in the hydrated state. Therefore, if all of the lipid was intracellular, which it almost certainly is not, the loss of this lipid upon histological processing would not be enough to account for the 50% shrinkage in fiber size that was observed. The labile substance lost from the dystrophic fibers with fixation and staining has not been determined, but it could well be water. If many of the dystrophic muscle fibers are swollen with water, they must also contain osmotically active particles to keep the water within the cells. These particles could be protein or ions that are not free to penetrate the cell membrane such as sodium which has been found in increased

amounts within the dystrophic muscle fiber (Baker et al., 1958 and Young et al., 1959).

It has been observed that the mean resting potential is lower and the mean fiber size larger in the dystrophic mice compared to their normal littermates. This raised the question as to whether in the dystrophic mice the large fibers had also low resting potentials. Graphs #5 and 10 show the resting potential plotted against the electrically determined fiber chord for each normal and dystrophic muscle fiber. It can be seen from Graph #10 that the dystrophic fibers with low resting potentials (under 80mv.) are generally smaller than the average dystrophic fiber (68u.). Therefore, the dystrophic fibers with less than average chord size (less than 68u.) were studied separately. Examination of these fibers revealed that there were two statistically different groups (see Graph #16). One group with resting potentials greater than 80mv. corresponded quite closely to the fibers found in normal mice. This group had a mean resting potential of 93.6 ± 7.7mv. (S.D.). The other group of fibers whose resting potential was less than 80mv. had a mean resting potential of 61.3 ± 12.8mv. (S.D.). If the two groups of fibers are combined, the mean resting potential of all dystrophic fibers less than 68u. in chord size was 81.7 ± 18.6mv. (S.D.). This differs only slightly from the mean of all dystrophic fibers which is 84.9 ± 15.9mv. (S.D.). From this it is apparent that the dystrophic muscle is composed of

three groups of fibers. Some fibers have a normal size (less than 68u.) and a normal resting potential (greater than 80mv.). Some are very much larger than normal but still maintain a normal resting potential. A third group of dystrophic fibers is nearly equal to the normal fibers in size but has a markedly reduced resting potential. It, therefore, seems likely that as the disease progressively affects the muscle fiber, it first swells but maintains its normal resting potential; and only later as the fiber shrinks to a more normal size does its resting potential fall.

From the electrical and histological data collected in this study, it was possible to make some estimates of *in vivo* and histological fiber and extra-fiber spaces. In the normal mouse there was a huge shrinkage of the extra-fiber space to 17% of its *in situ* (electrically determined) value with histological processing. This occurred while the mean fiber chord size changed only slightly. The shrinkage of the extra-fiber space resulted in an apparent increase in the histological mean % fiber space. However as the mean fiber chord size did not change, the increased fiber space is probably artifactual. The extra-fiber space from the electrical measurements is 78% for normal mice gastrocnemius muscles *in situ*. This does not agree with 28% obtained by Creese, Scholes, and Whalen (1958) for excised stretched rat diaphragm. Neither does it agree with the inulin space of

28% quoted by them. Tasker et al. (1959) found that the extracellular space of the excised toad sartorius muscle varied from 8 to 40% using inulin and sucrose determinations. They also found a decrease in extra-fiber space with an increase in the fiber size. The differences noted here may be due to species variability, changes from the in situ to the excised condition, variations in muscle tension, differences between muscles in the same animal, or inaccuracies in the various techniques used. Further investigation of these discrepancies seems warranted.

In the dystrophic muscles even though the average fiber size was twice as large as normal, the fiber space and extra-fiber space was nearly the same as in the normal muscles. This was because fewer fibers of larger size were present per unit volume in the dystrophic muscles. The larger histologically determined fiber space in the normal muscles compared to that in the dystrophic muscles was due to the fiber chord shrinkage which reduced the fiber space in the fixed dystrophic muscles. It will be seen from Table VII that the extra-fiber space was reduced slightly less in the dystrophic muscles than in the normal ones after histological processing. This is probably due to the increased connective tissue present in these muscles.

From the data presented here, it becomes apparent that the true geographical distribution of muscle fibers is not what is seen on histological sections where all of the fibers

of a fasciculus are packed tightly together. Rather the fibers appear to be spread apart and separated by fairly large "spaces" in the living state. With histological preparation these "spaces" collapse while the normal fibers maintain their *in situ* size. In terms of the electrical properties of muscle fibers this seems logical because the large extra-fiber spaces would tend to isolate one fiber from another. If on the other hand what is seen histologically were true *in situ*, there would be a spread of electrical currents from fiber to fiber; and the whole fasciculus would respond as a unit. Histological studies of muscles without fixation and dehydration were attempted using frozen section and freeze-dry techniques. However, these were unsuccessful. Further investigation of muscle fiber relationships in the living animal should be undertaken in order to better understand both the physical arrangement and electrical interaction of muscle fibers.

CONCLUSIONS

1. Using motor driven microelectrodes, the resting potentials of the gastrocnemius muscle fibers in living normal and dystrophic mice were measured. The muscle fiber sizes and geographical distribution were determined *in vivo* and compared to similar histological data for both groups of mice.

2. The *in situ* mean resting potential of 92.5mv. in normal mice is significantly larger than the mean resting potential of 84.9mv. observed in living dystrophic mice. These values approximate those predicted from the Nernst Equation.

3. Evidence is presented that a layer of negatively charged particles may be present on the inside of the normal cell membrane.

4. The mean fiber chord of 67.9u. found in living dystrophic mice is significantly larger than the mean fiber chord of 34.8u. observed in living normal mice. The mean fiber chord determined from histological sections is not different (32.7u. and 32.8u.) for the two groups of mice.

5. In the dystrophic mice low resting potentials were associated with fibers of relatively normal size.

6. In the dystrophic mice it is probable that as the disease progresses, first the affected fibers swell but maintain a normal resting potential; and later they are reduced in size and gradually lose their resting potential. A proportion of fibers in any dystrophic muscle is of normal size and has a normal resting potential.

7. The large size of some of the *in situ* dystrophic muscle fibers may be due to the accumulation of water and non-diffusible particles within the cell membrane which are lost upon histological processing.

8. In the normal mouse muscle there is a loss of about 80% of the extra-fiber space with histological preparation while the average fiber size changes only slightly. In the dystrophic mouse muscle the average fiber size shrinks more than 50% while the extra-fiber space is reduced nearly 80% with histological processing.

9. The histological section of a muscle probably does not give a true picture of the fiber relations. In the living muscle relatively large spaces seem to separate the fibers. These spaces appear to vary with species, muscle, tension, and method of measurement.

BIBLIOGRAPHY

1. Adams, R.D., Denny-Brown, D., and Pearson, C. *Disease of Muscle*. New York, Paul B. Hoeber, Inc., 1954.

2. Adrian, R.H. The effect of internal and external potassium concentration on the membrane potential of frog muscle. J. Physiol., 1956, 133:631-658.

3. Baker, N., Blahd, W., and Hart, P. Concentration of K and Na in skeletal muscle of mice with a hereditary myopathy (*Dystrophia Muscularis*). Am. J. of Physiol., 1958, 193:530-533.

4. Banker, B.Q. and Denny-Brown, D. A study of dennervated muscle in normal and dystrophic mice. J. Neuropath. & Exp. Neurol., 1959, 18:517-530.

5. Bennett, A.L., Ware, F., Dunn, A.L. and McIntyre, A.R. The normal membrane resting potential of mammalian skeletal muscle measured *in vivo*. J. Cell. & Comp. Physiol., 1953, 42:343-357.

6. Blum, J.L., Creese, R., Jenden, D.J., and Scholes, N. The mechanism of action of ryanodine on skeletal muscle. J. Pharm. & Exp. Therapeutics, 1957, 121:477-486.

7. Boyd, I.A. and Martin, A.R. Spontaneous subthreshold activity at mammalian neuromuscular junctions. J. Physiol., 1956, 132:61-73.

8. Brooks, S., Giese, A.C. and Giese, R.I. Potential differences across natural membranes separating unlike salt solutions. J. of Exp. Biol., 1931, 8:124-132.

9. Choh-Luh Li, G., Shy, M., Wells, J. Some properties of mammalian skeletal muscle fibers with particular reference to fibrillation potentials. J. Physiol., 1957, 135:522-535.

10. Creese, R. Measurement of cation fluxes in rat diaphragm. Proc. Roy. Soc. of London, 1954, 142B:497-513.

11. Creese, R., Dillon, J.P., Marshall, J., Sabawala, D.J., Schneider, D.J., Taylor, D.B., and Zinn, D.E. The effect of neuromuscular blocking agents on isolated human intercostal muscles. J. Pharm. & Exp. Therapeutics, 1957, 119:485-494.

12. Creese, R., Scholes, N.W., and Whalen, W.J. Resting potentials of diaphragm muscle after prolonged anoxia. J. Physiol., 1958, 140:301-317.

13. Emerson, J.D. and Emerson, G.M. Comparison of gastrocnemius fiber diameters among mammalian species. Fed. Proc., 1959, 18:42.

14. Fetterman, G.H., Wratney, M.J., Donaldson, J.S., and Danowski, T.S. Muscular dystrophy -- history, clinical status, muscle strength, and biopsy findings. A.M.A. Am. J. of Dis. of Children, 1956, 91:326-338.

15. Geiger, R.S. and Garvin, J.S. Pattern of regeneration of muscle from progressive muscular dystrophy patients cultivated in vitro as compared to normal human skeletal muscle. J. of Neuropath. & Exp. Neurol., 1957, 16:532-543.

16. Gerard, R.W. and Ling, G. Membrane potential of single muscle fibers. Am. J. of Physiol., 1948, 155:437-438.

17. Graham, J. and Gerard, R.W. Membrane potentials and excitation of impaled single muscle fibers. J. Cell. & Comp. Physiol., 1946, 28:99-117.

18. Hodgkin, A.L. and Huxley, A.F. Action potentials recorded from inside a nerve fiber. Nature, 1939, 144:710-711.

19. Hodgkin, A.L. and Huxley, A.F. Resting and action potentials in single nerve fibers. J. Physiol., 1945, 104:176-195.

20. Jenerick, H.P. The relation between prepotential, resting potential, and latent period in frog muscle fibers. J. Gen. Physiol., 1956, 39:773-787.

21. Jenerick, H.P. and Gerard, R.W. Membrane potential and threshold of single muscle fibers. J. Cell. & Comp. Physiol., 1953, 42:79-102.

22. Kurella, G.A. Methods of studying the changes in the resting potential of single muscle fibers. Biophysics, 1958, 3:358-364.

23. Liley, A.W. An investigation of spontaneous activity at the neuromuscular junction of the rat. J. Physiol., 1956, 132:650-666.

24. Ling, G. New hypothesis for the mechanism of cellular resting potential. Fed. Proc., 1955, 14:302.

25. Ling, G. Muscle electrolytes. Am. J. of Phys. Med., 1955, 34:89-101.

26. Ling, G. and Gerard, R.W. The membrane potential and metabolism of muscle fibers. J. Cell. & Comp. Physiol., 1949, 34:413-438.

27. Ling, G. and Gerard, R.W. External potassium and the membrane potential of single muscle fibers. Nature, 1950, 165:113-114.

28. Ling, G. and Schmolinske, A. Further evidence for the fixed charge hypothesis. Fed. Proc., 1956, 15:391.

29. McIntyre, A.R., Bennett, A.L., and Hinman, J.S. Filbrillation in dystrophic muscle. Physiologist, 1957, 1:59.

30. McIntyre, A.R., Bennett, A.L., and Brodkey, J.S. Muscle dystrophy in mice of the Bar Harbor strain. A.M.A. Arch. of Neurol. & Psych., 1959, 81:678-683.

31. Michelson, A.M., Russell, E.S., and Harmon, P.J. Dystrophis muscularis: A hereditary primary myopathy in the house mouse. Proc. Nat. Acad. of Sciences, 1955, 41:1079-1084.

32. Milhorat, A.T. The diagnosis of muscular dystrophy. Am. J. of Phys. Med., 1955, 34:103-108.

33. Nastuk, W. Neuromuscular transmission. Am. J. of Med., 1955, 19:663-668.

34. Nastuk, W. and Alexander, J. An instrument for the production of microelectrodes used in electrophysiological studies. Rev. of Scientific Instruments, 1953, 24:528-531.

35. Nastuk, W. and Hodgkin, A.L. The electrical activity of single muscle fibers. J. Cell. & Comp. Physiol., 1950, 35:39-73.

36. Shanes, A.M. Electrochemical aspects of physiological and pharmacological action in excitable cells. Part I. The resting cell and its alteration by extrinsic factors. Pharm. Rev., 1958, 10:59-164.

37. Shank, R.E., Gilder, H., and Hoagland, C.L. Studies on diseases of muscle. Part I. Progressive muscular dystrophy; a clinical review of forty cases. Arch. of Neurol. & Psych., 1944, 52:431-442.

38. Shaw, F.H., Simon, S.E., and Johnstone, B.M. The non-correlation of bioelectric potentials with ionic gradients. J. Gen. Physiol., 1956, 40:1-17.

39. Spector, W.S. Handbook of Biological Data, p. 294. Philadelphia, W.B. Saunders Co., 1956.

40. Tasker, P., Simon, S.E., Johnstone, B.M., Shankly, K.H., and Shaw, F.H. The dimensions of the extracellular space in sartorius muscle. J. Gen. Physiol., 1959, 43:39-53.

41. Timiras, P.S., Woodbury, D.M., and Goodman, L.S. Effect of adrenalectomy, hydrocortisone acetate, and desoxycorticosterone acetate on brain excitability and electrolyte distribution in mice. J. Pharm. & Exp. Therapeutics, 1954, 112:80-93.

42. Tyler, F.H. Studies in disorders of muscle Part III. Pseudohypertrophy of muscle in progressive muscular dystrophy and other neuromuscular diseases. Arch. of Neurol. & Psych., 1950, 63:425-432.

43. Tyler, F.H. and Wintrobe, M.M. Studies in disorders of muscle Part I. The problem of progressive muscular dystrophy. Ann. of Int. Med., 1950, 32:72-79.

44. Underwood, B.J., Duncan, C.P., Taylor, J.A., Cotton, J.W. Elementary Statistics. New York, Appleton-Century-Croft, Inc., 1954.

45. Walton, J.N. and Adams, R.D. The response of the normal, the denervated, and the dystrophic muscle cell to injury. J. of Path. & Bact., 1956, 72:273-298.

46. West, W.T. and Mason, K.E. Degeneration and regeneration in experimental muscular dystrophy. Am. J. of Phys. Med., 1955, 35:223-239.

47. Young, H.L., Young, W., and Edelman, I.S. Electrolyte and lipid composition of skeletal and cardiac muscle in mice with hereditary muscular dystrophy. Am. J. of Physiol., 1959, 197:487-490.

Table I. Resting Potentials and Fiber Chords of Normal Mice Muscles.

Muscle Number	Average Resting Potential & S.D.	Average Electrical Fiber Chord & S.D.	Average Histologic Fiber Chord
# 14	89.6 ± 12.4mv.	29.1 ± 15.2u.	28.6u.
15	91.0 ± 8.2	32.9 ± 14.7	32.7
16B	89.3 ± 11.1	30.8 ± 13.9	34.4
17	94.3 ± 5.7	39.6 ± 21.6	36.7
37	98.4 ± 3.7	36.4 ± 17.6	29.1
38	96.0 ± 15.1	44.6 ± 25.8	34.7
Mean	92.5 ± 10.8mv.	34.8 ± 19.2u.	32.7 ± 15.9u.
	N = 298	N = 297	N = 837

Table II. Electrically Determined Fiber and Extra-fiber Spaces of Normal Mice Muscles.

Muscle Number	Total Distance	Fiber Space	Extra-fiber Space	% Fiber Space	% Extra-fiber Space
# 14	7840u.	1459u.	6381u.	19%	81%
15	7875	1431	6444	18%	82%
16B	7875	2124	5751	27%	73%
17	7875	2536	5339	32%	68%
37	7875	1309	6566	17%	83%
38	7875	1516	6359	19%	81%
Mean	7869u.	1729u.	6140u.	22% ± 5.5%	78% ± 5.5%

Table III. Histologically Determined Fiber and Extra-fiber Spaces of Normal Mice Muscles.

Muscle Number	Total Distance	Fiber Space	Extra-fiber Space	% Fiber Space	% Extra-fiber Space
# 14	6490u.	3260u.	3230u.	50%	50%
15	7350	4575	2775	62%	38%
16B	7800	4643	3157	60%	40%
17	7300	4849	2451	66%	34%
37	7580	4649	2931	61%	39%
38	7633	5419	2214	71%	29%
Mean	7526u.	4566u.	2793u.	62.0% ± 7.6%	38.0% ± 7.6%

Table IV. Resting Potentials and Fiber Chords of Dystrophic Mice Muscles.

Muscle Number	Average Resting Potential & S.D.	Average Electrical Fiber Chord & S.D.	Average Histologic Fiber Chord
# 31	83.6 ± 11.2mv.	64.6 ± 39.4u.	36.7 ± 15.8u.
32B	71.0 ± 18.5	62.4 ± 46.3	30.8 ± 14.2
33	89.6 ± 17.8	59.6 ± 42.3	37.1 ± 16.5
35	89.8 ± 6.3	67.8 ± 48.0	38.7 ± 18.7
35B	80.1 ± 12.6	71.5 ± 50.1	29.1 ± 13.7
36	93.4 ± 13.0	78.0 ± 63.1	28.7 ± 12.2
Mean	84.9 ± 15.9mv.	67.9 ± 49.1u.	32.8 ± 16.0u.
	N = 166	N = 166	N = 737

Table V. Electrically Determined Fiber and Extra-fiber Spaces of Dystrophic Mice Muscles.

Muscle Number	Total Distance	Fiber Space	Extra-fiber Space	% Fiber Space	% Extra-fiber Space
# 31	9520u.	2002u.	7518u.	21%	79%
32B	8015	1123	6892	14%	86%
33	8085	1073	7012	13%	87%
35	9905	2846	7059	29%	71%
35B	6825	2359	4466	35%	65%
36	6300	1871	4429	30%	70%
Mean	8108u.	1879u.	6288u.	24% ± 7.3%	76% ± 7.3%

Table VI. Histologically Determined Fiber and Extra-fiber Spaces of Dystrophic Mice Muscles.

Muscle Number	Total Distance	Fiber Space	Extra-fiber Space	% Fiber Space	% Extra-fiber Space
# 31	8015u.	3342u.	4673u.	42%	58%
32B	6987	2463	4524	35%	65%
33	7540	3192	4348	42%	58%
35	13473	5495	7978	41%	59%
35B	11527	5276	6251	46%	54%
36	10025	4504	5498	45%	55%
Mean	9591u.	4035u.	5556u.	42.1% ± 3.4%	57.9% ± 3.4%

Table VII. Comparison of Normal and Dystrophic Mice Muscles.

		Normal Muscles	Dystrophic Muscles
1.	Mean Resting Potential	92.5 ± 10.8mv.	84.9 ± 15.9mv.
2.	Electrically Determined Mean Fiber Chord	34.8 ± 19.2u.	67.9 ± 49.1u.
3.	Histologically Determined Mean Fiber Chord	32.7 ± 15.9u.	32.8 ± 16.0u.
4.	Electrically Determined % Fiber Space	22% ± 5.5%	24% ± 7.3%
5.	Electrically Determined % Extra-fiber Space	78% ± 5.5%	76% ± 7.3%
6.	Histologically Determined % Fiber Space	62% ± 7.6%	42% ± 3.4%
7.	Histologically Determined % Extra-fiber Space	38% ± 7.6%	58% ± 3.4%
8.	Ratio of Electrical to Histological Extra-fiber Space	5.8 / 1	4.6 / 1
9.	% Fiber Shrinkage	6%	53%
10.	% Extra-fiber Space Shrinkage	83%	78%
11.	Number of Fibers Studied Electrically	297	166
12.	Number of Fibers Studied Histologically	837	737

Graph #1

Frequency Distribution of Voltages at 35u. Intervals Through Normal Mouse Muscle

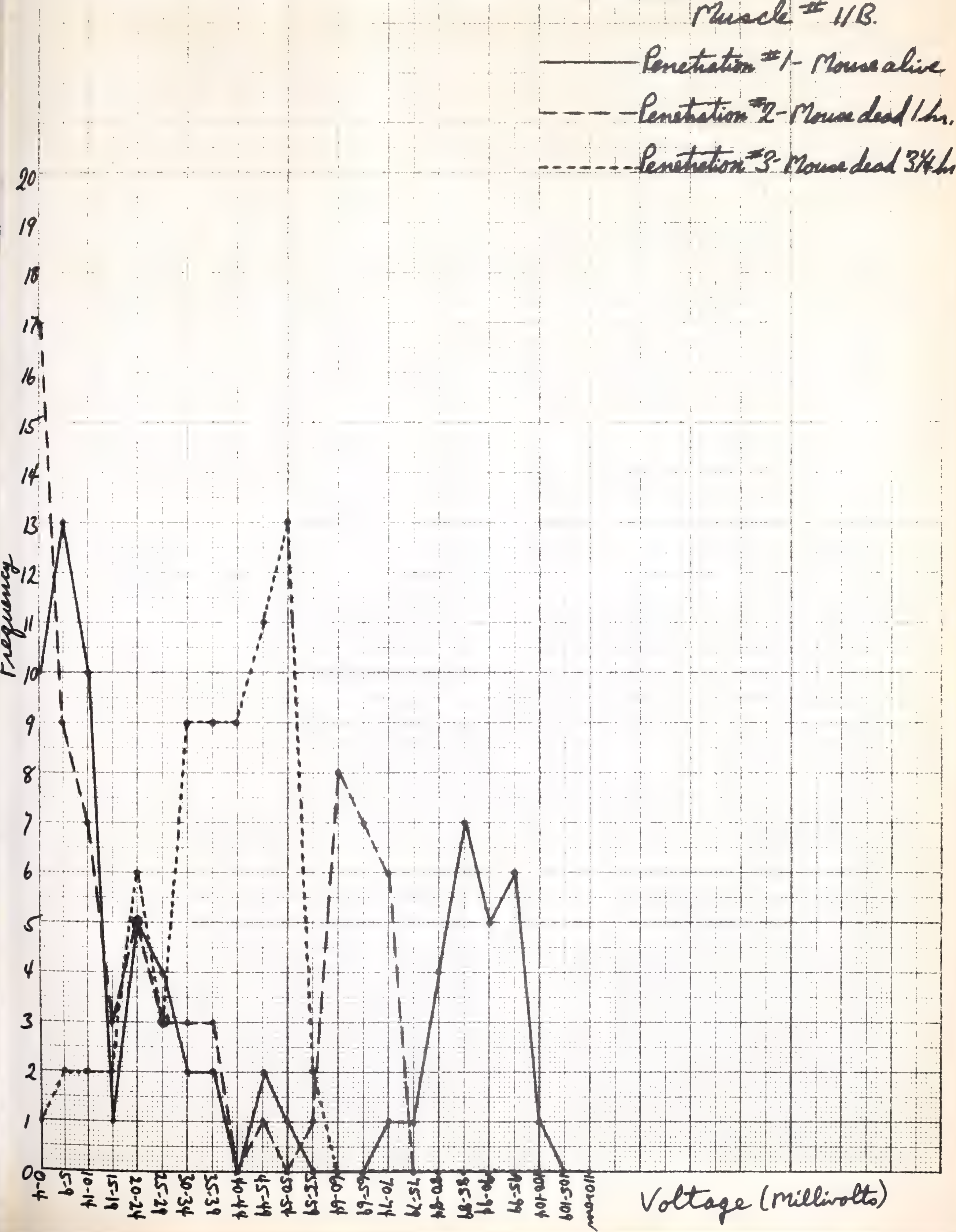

Graph #2

Frequency Distribution of Voltages at 35μ Intervals Through Normal Mice Muscles.

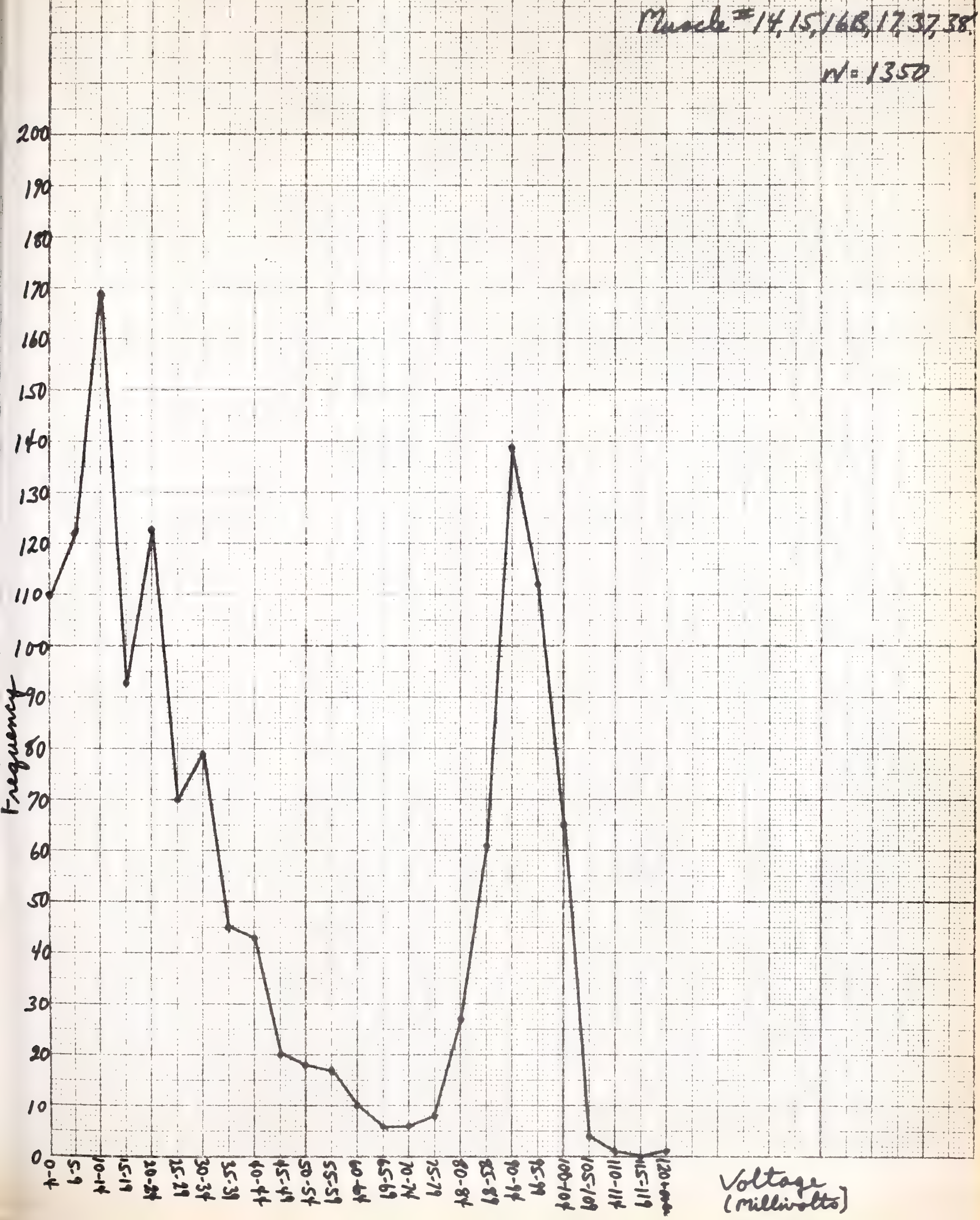

Graph #3

Frequency Distribution of Resting Potentials in Normal Mouse Gastrocnemius Muscles.

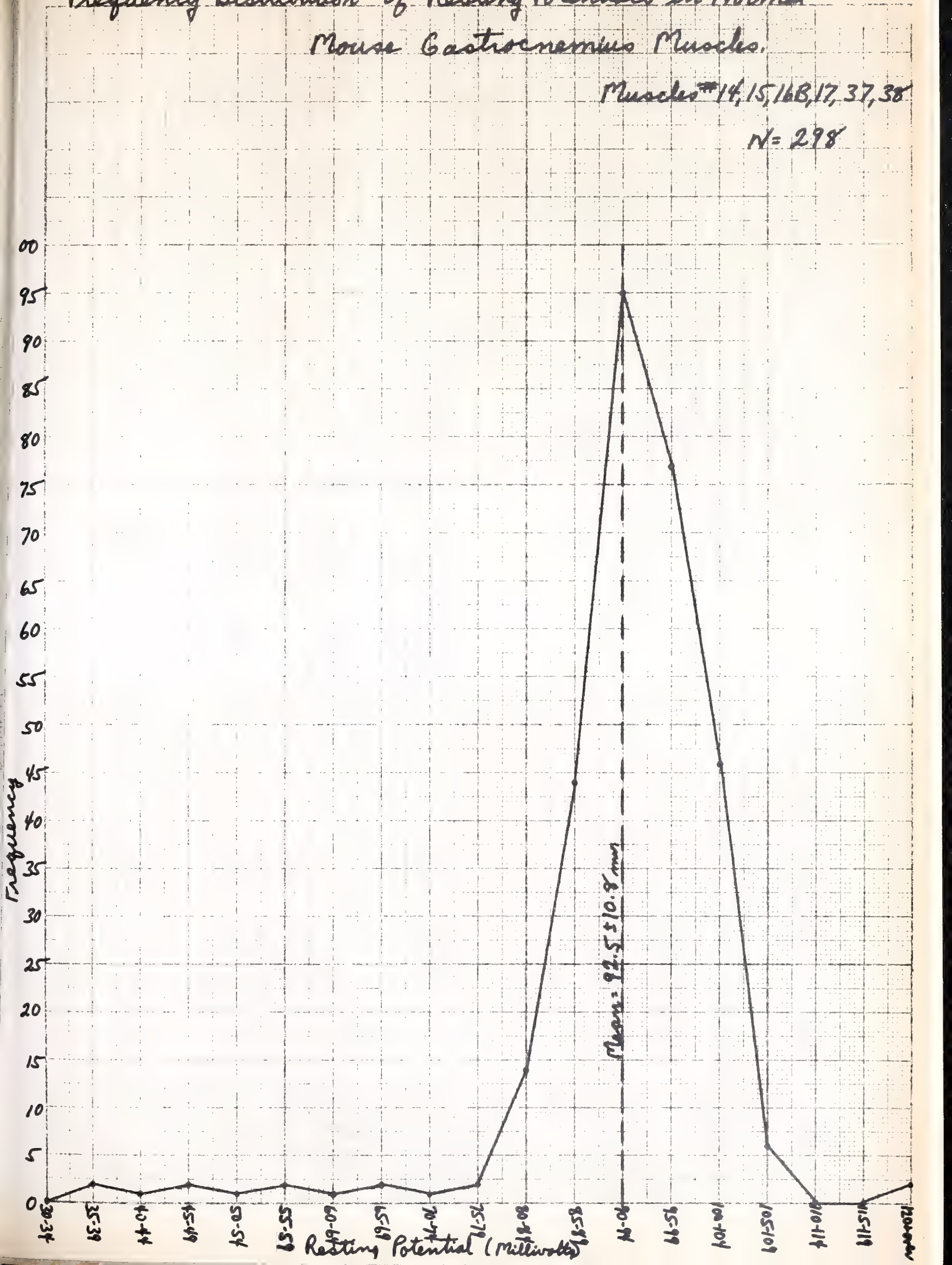

Muscles # 14, 15, 16B, 17, 37, 38

N= 298

Graph #4

Frequency Distribution of Electrically Determined Fiber Chords in Normal Mice Muscles

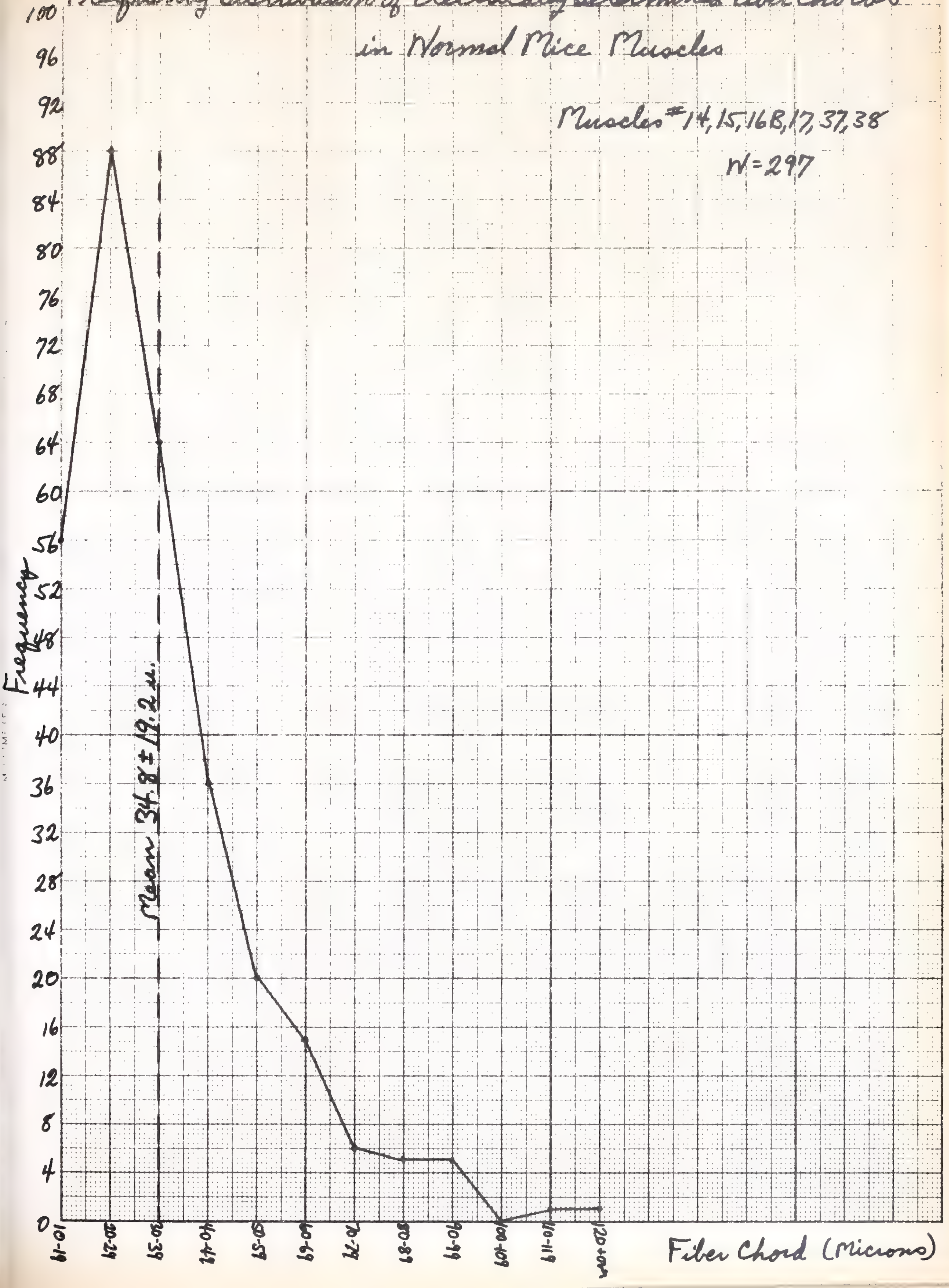

Graph #5

Resting Potential Compared to Fiber Chord in Normal Mice Muscle

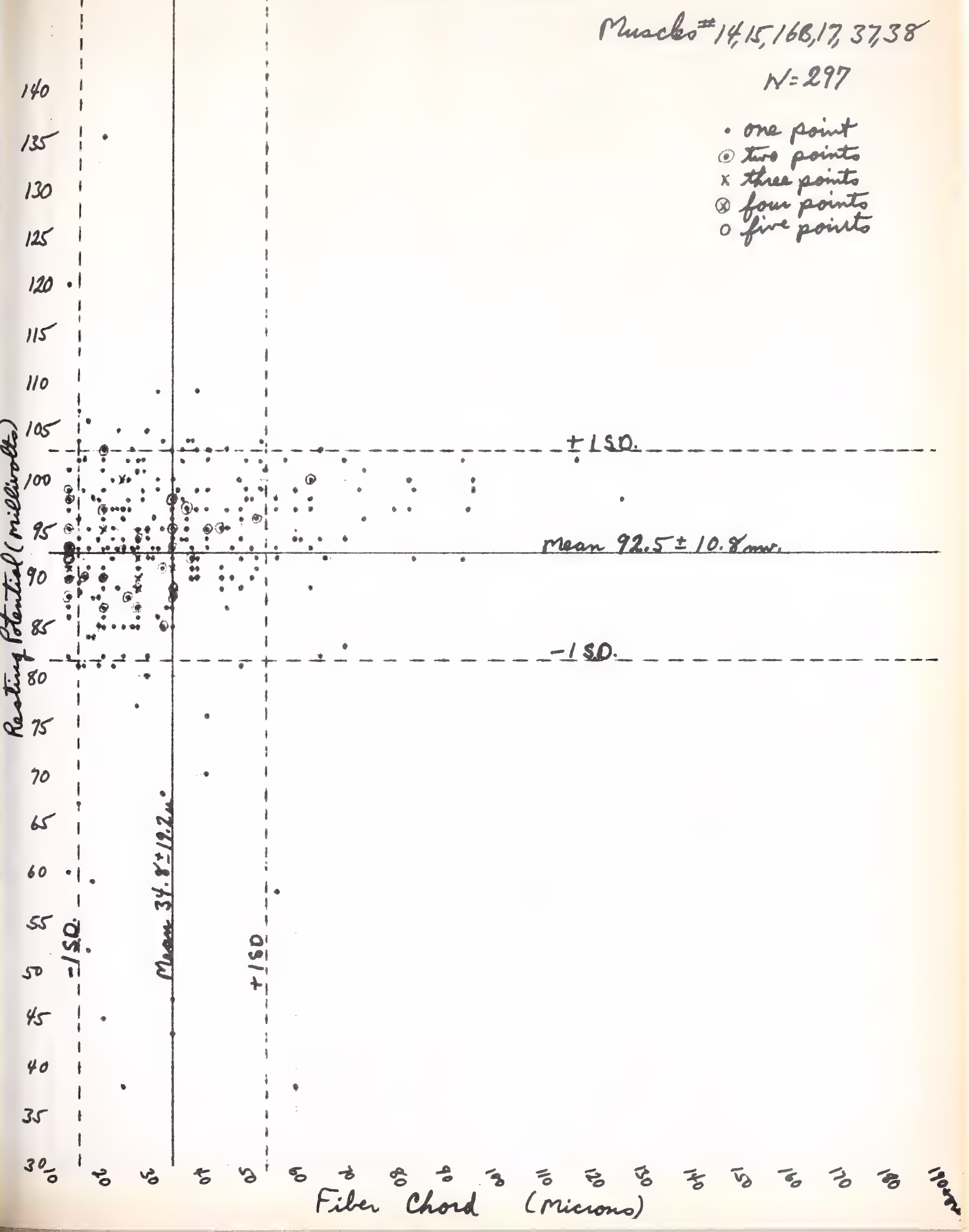

Graph #6

Frequency Distibution of Histologically Determined Fiber Chords in Normal Mice Muscles

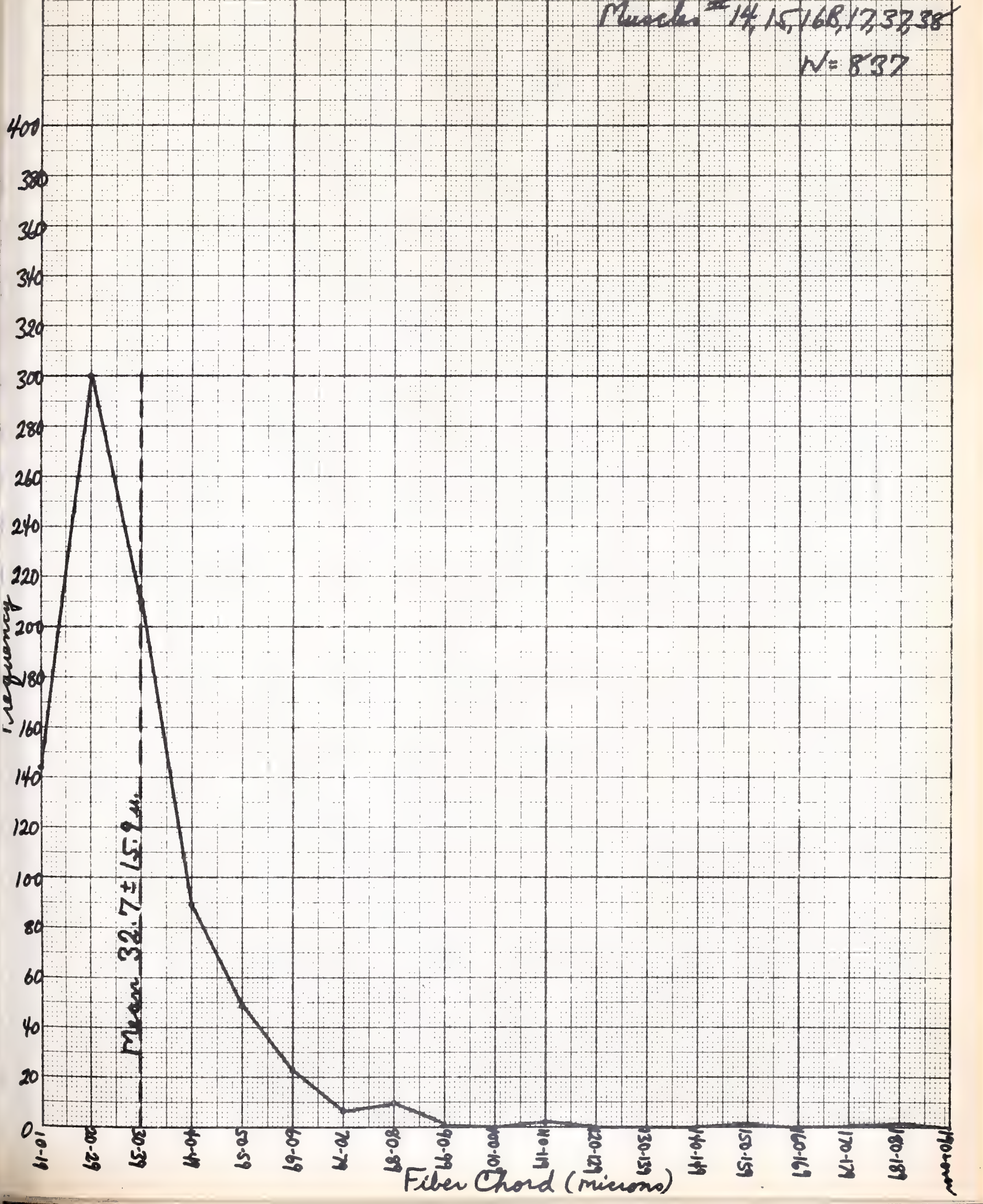

Graph #7

Frequency Distribution of Voltages at 35u Intervals Through Dystrophic Mice Muscles

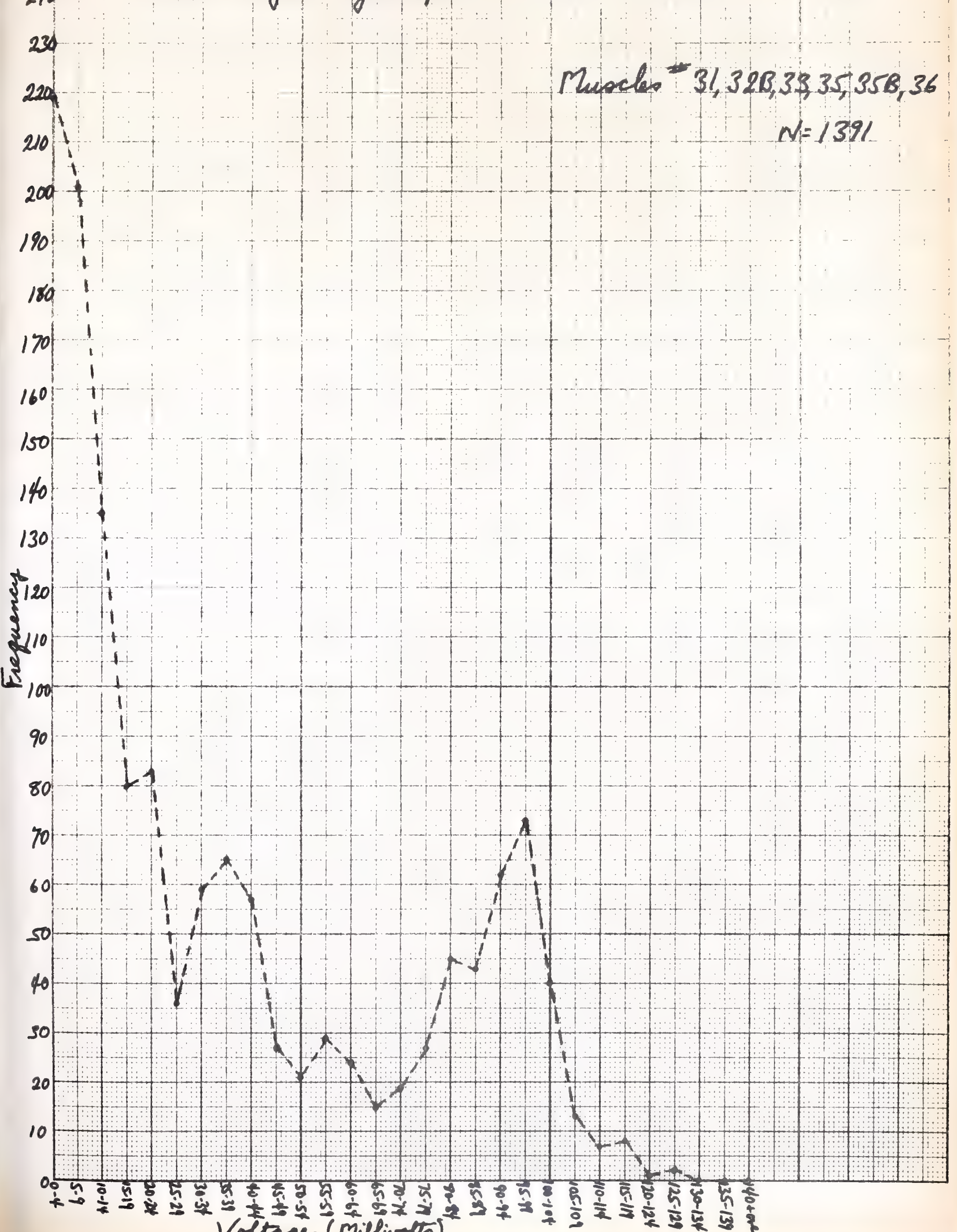

Graph #8

Frequency Distribution of Resting Potentials in Dystrophic Mice Muscles

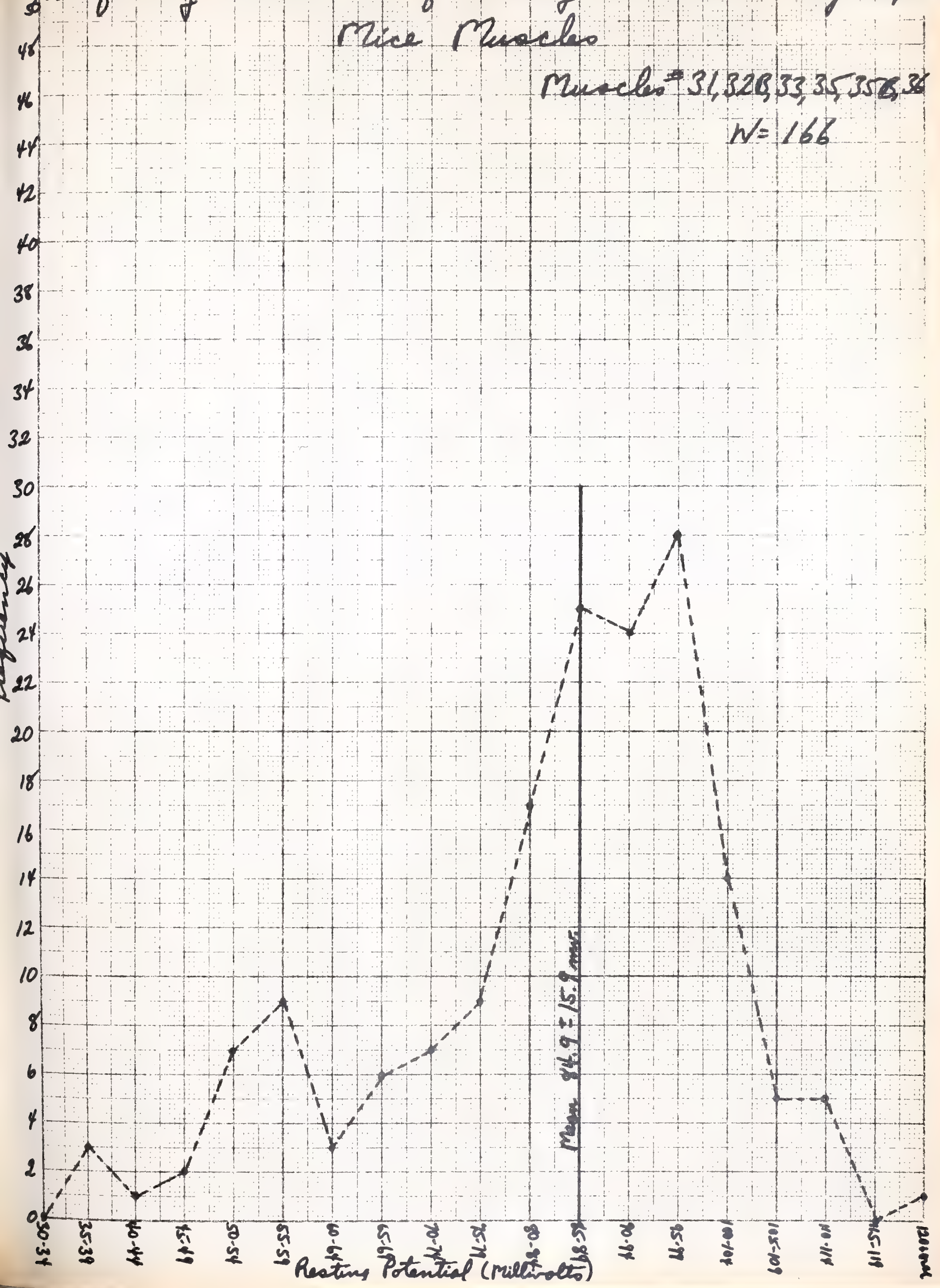

Muscles # 31, 32B, 33, 35, 35B, 36

N = 166

Mean 84.9 ± 15.9 mv.

Graph #9

Frequency Distribution of Electrically Determined Fiber Chords in Dystrophic Mice Muscles

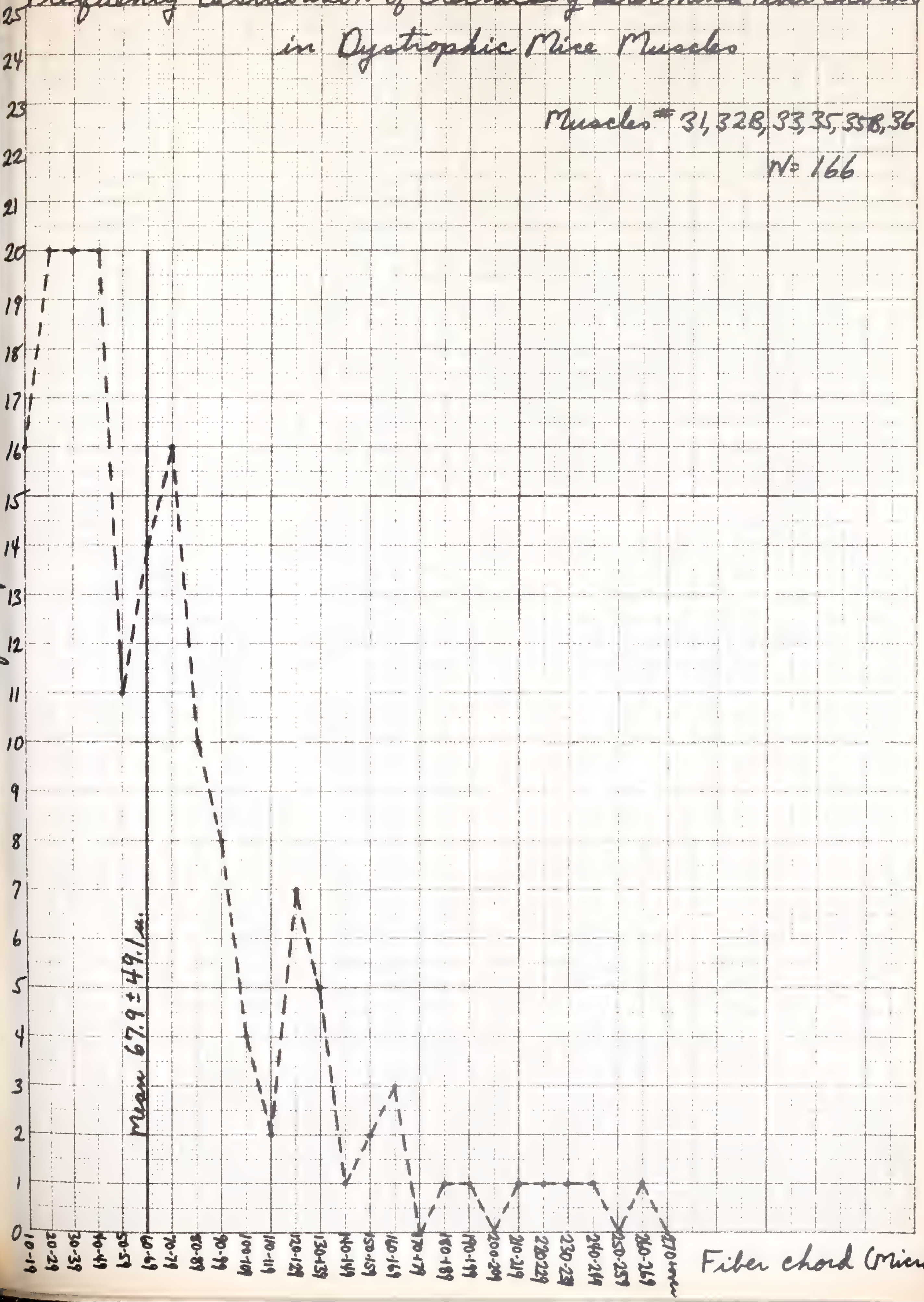

Graph #10

Resting Potential Compared to Fiber Chord in Dystrophic Mice Muscle

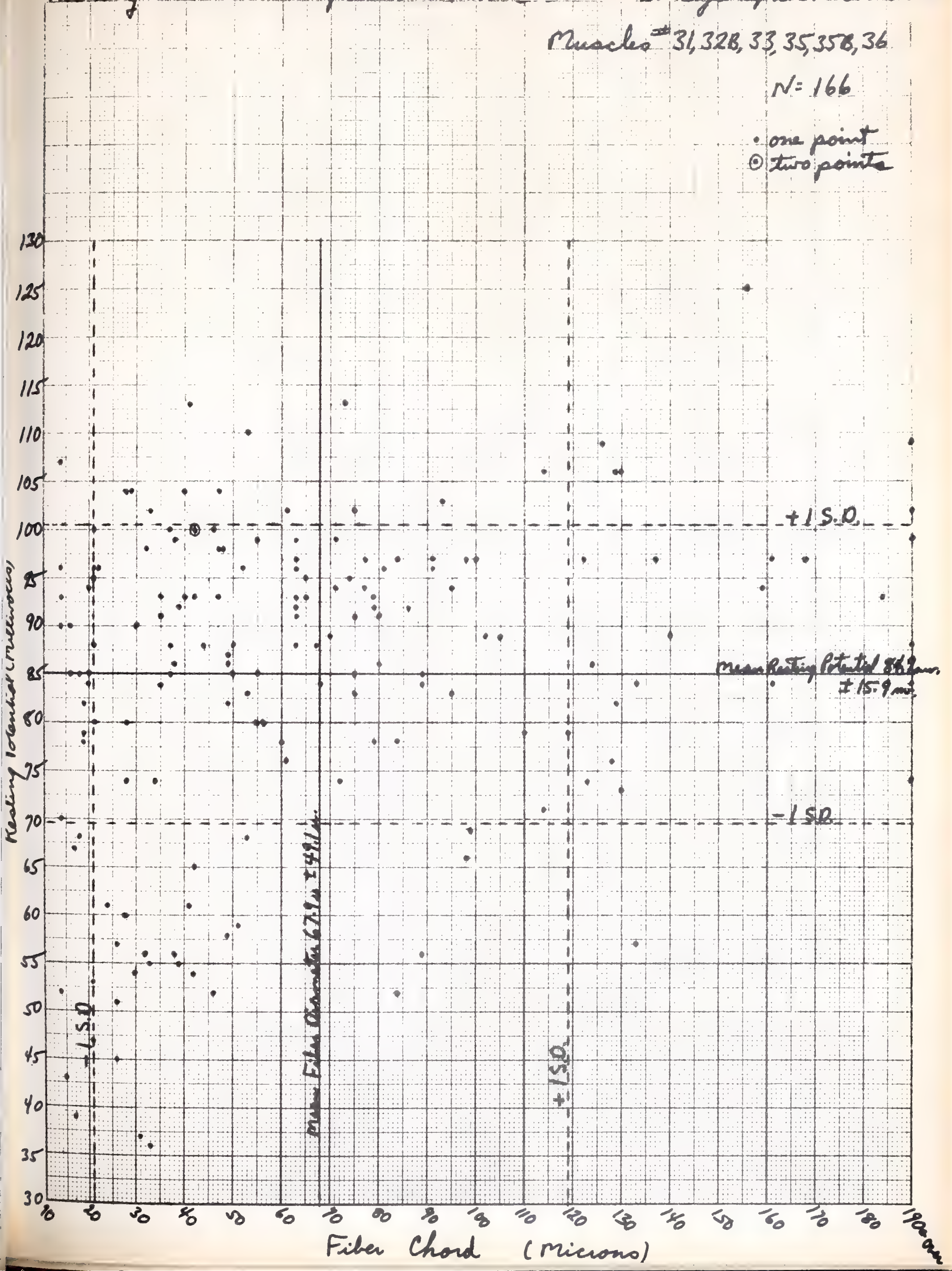

Graph #11

Frequency Distibution of Histologically Determined Fiber Chords in Dystrophic Mice Muscles

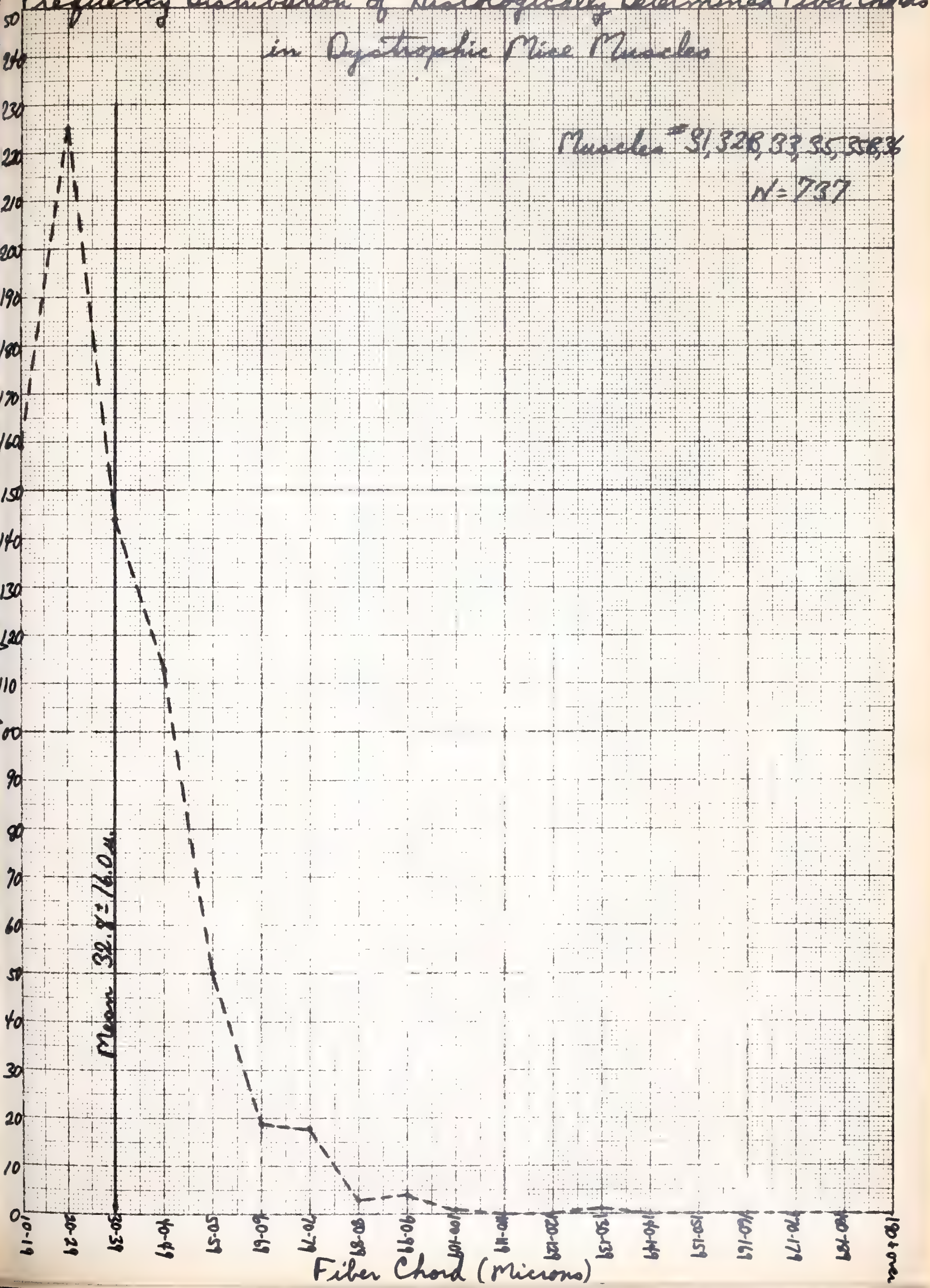

Graph #12

Frequency Distribution of Voltages at 35μ Intervals of Depth in Normal and Dystrophic Mice Muscles.

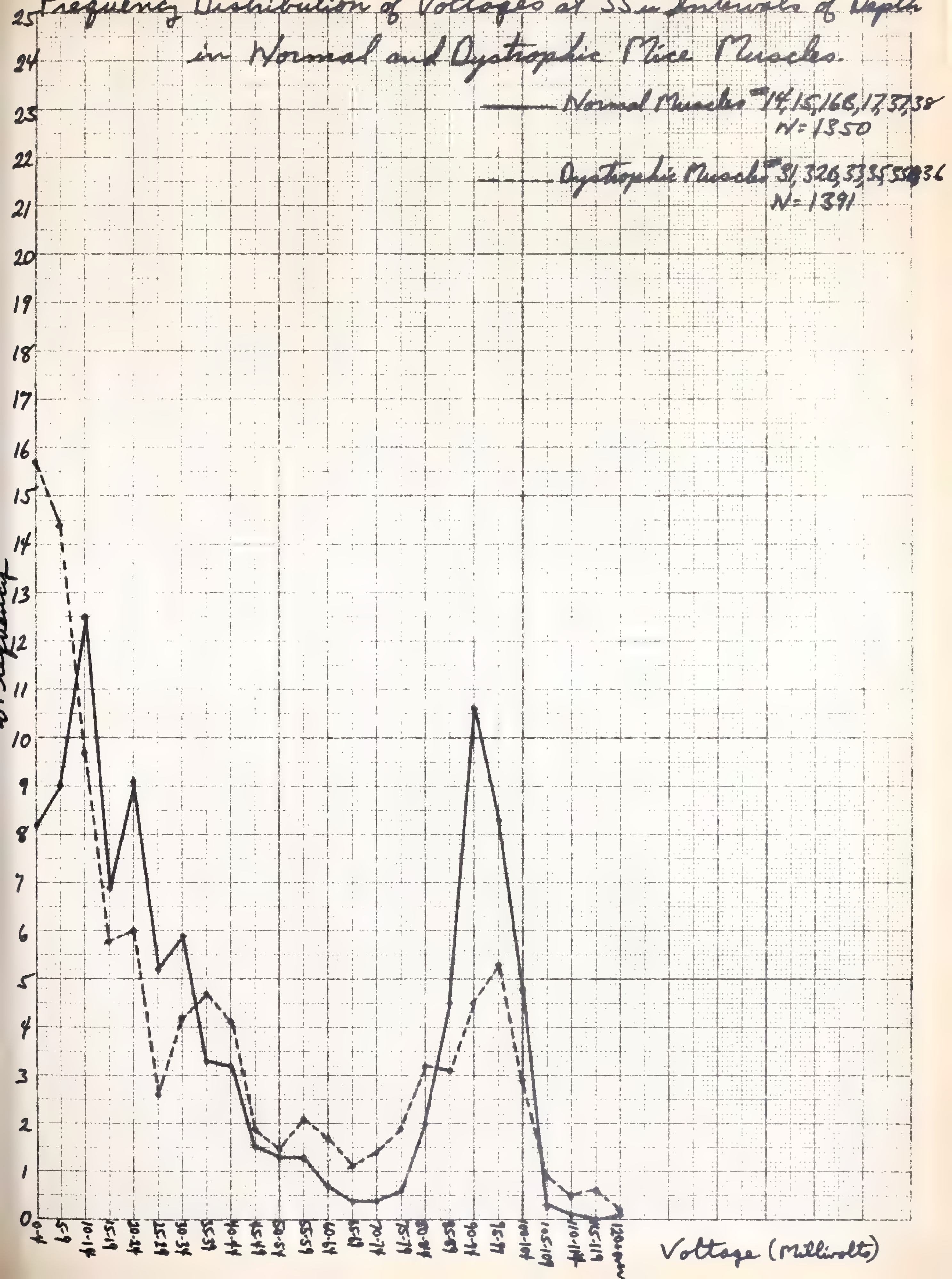

Graph #13

Frequency Distribution of Resting Potentials in Normal and Dystrophic Mice Muscles

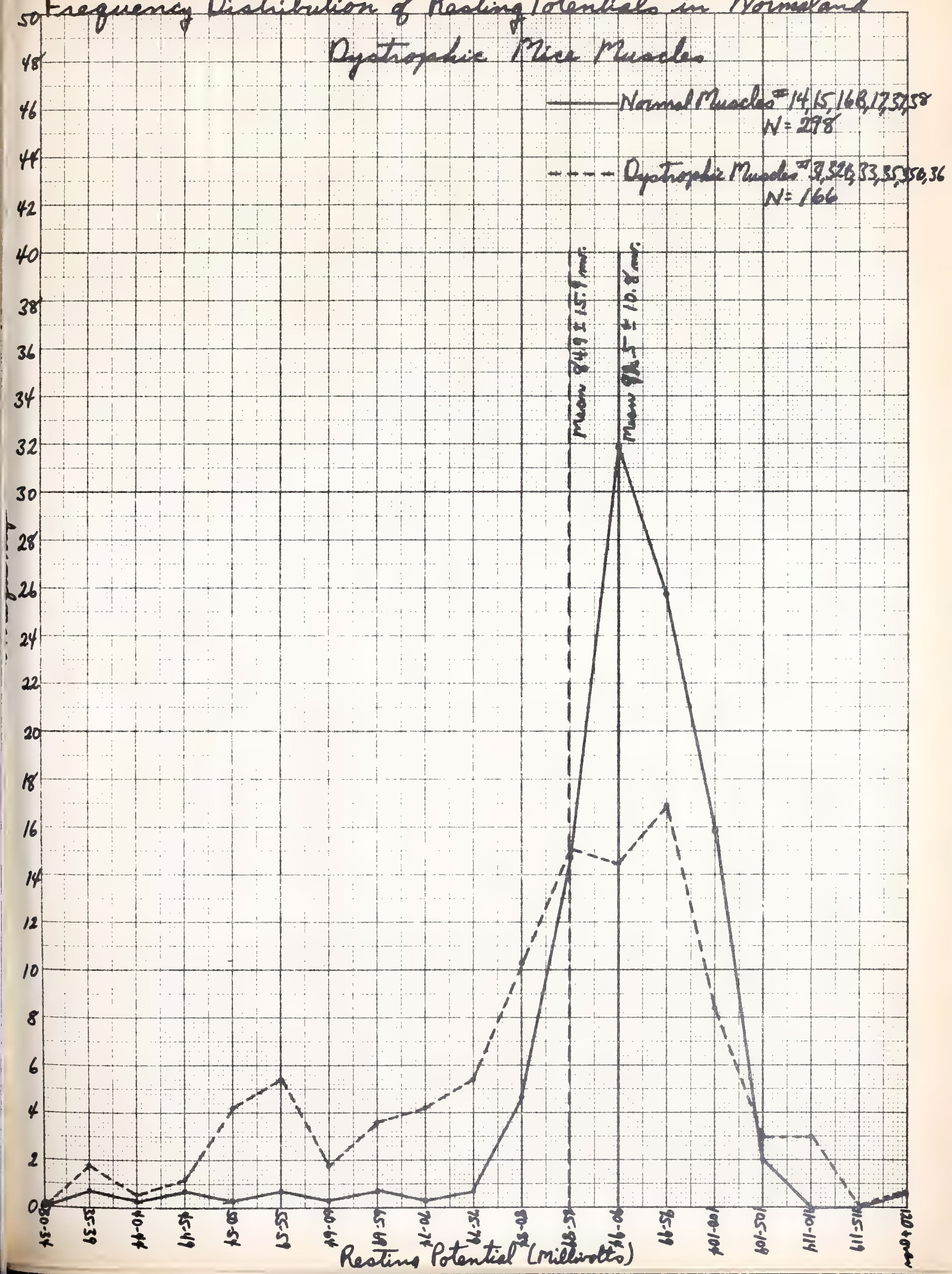

Graph #14

Frequency Distribution of Electrically Determined Fiber Chords in Normal and Dystrophic Mice Muscles

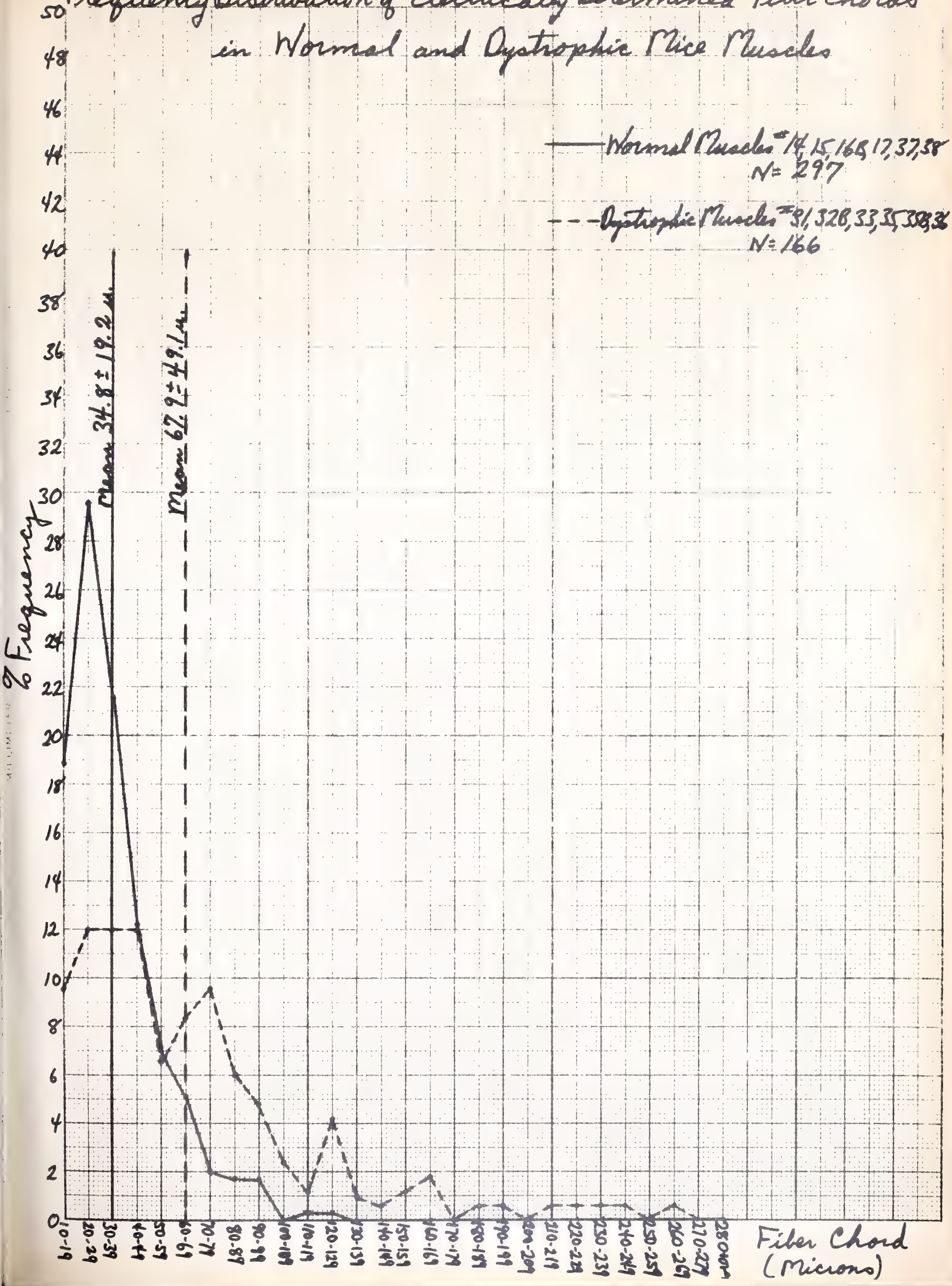

Graph #15

Frequency Distribution of Histologically Determined Fiber Chords in Normal and Dystrophic Mice Muscles

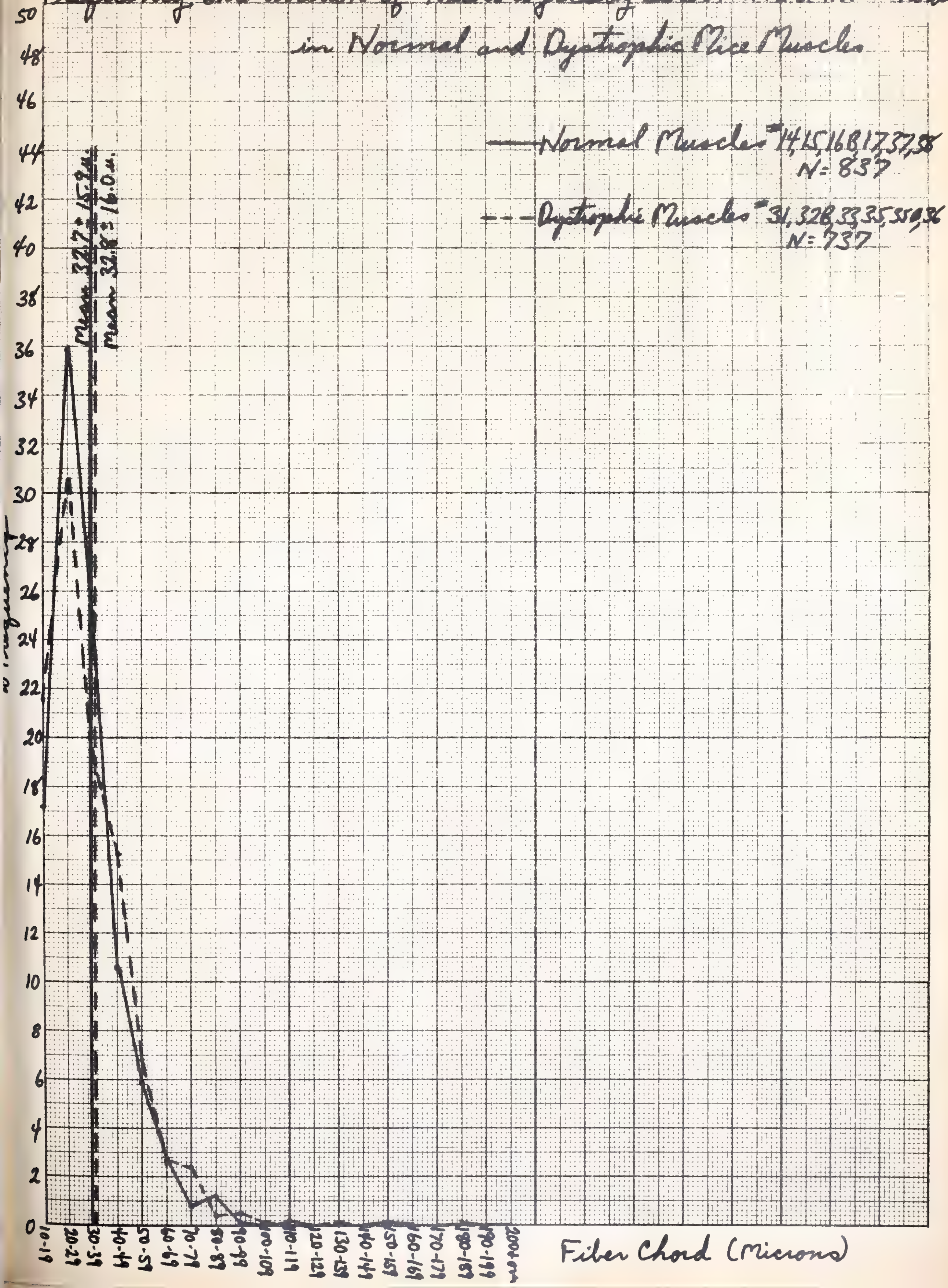

Graph #16

Frequency Distribution of Resting Potentials in Fibers Whose Chord Is Less Than 68u in Dystrophic Mice